

muscle fibers dramatically improved the contractile properties of dystrophic muscle. This improvement in contractile force was thought to be achieved by hyperphosphorylated microdystrophin-positive muscle fibers.

**RESULTS**

**Construction of an AAV-2 Vector Carrying Microdystrophin ΔCS1**

We constructed an AAV-2 vector encoding microdystrophin ΔCS1 under the control of a truncated, muscle-specific creatine kinase (MCK) promoter [15]. We designated this recombinant AAV vector AAV2-MCKΔCS1. CS1, which has the N-terminal, actin-binding domain, four rod repeats and three hinges, the cysteine-rich domain, and the C-terminal domain, effectively rescued dystrophic phenotypes when introduced as a transgene [14]. To shorten CS1 cDNA (4.9 kb) further, we deleted the 5' and 3' untranslated regions (UTRs) and exons 71–78 (alternative splicing regions of dystrophin mRNA) by PCR techniques. We named the resultant 3.8-kb cDNA ΔCS1 (Fig. 1).

**Expression of ΔCS1 Microdystrophin at the Sarcolemma after AAV2-MCKΔCS1-Mediated Gene Transfer into *mdx* Muscle**

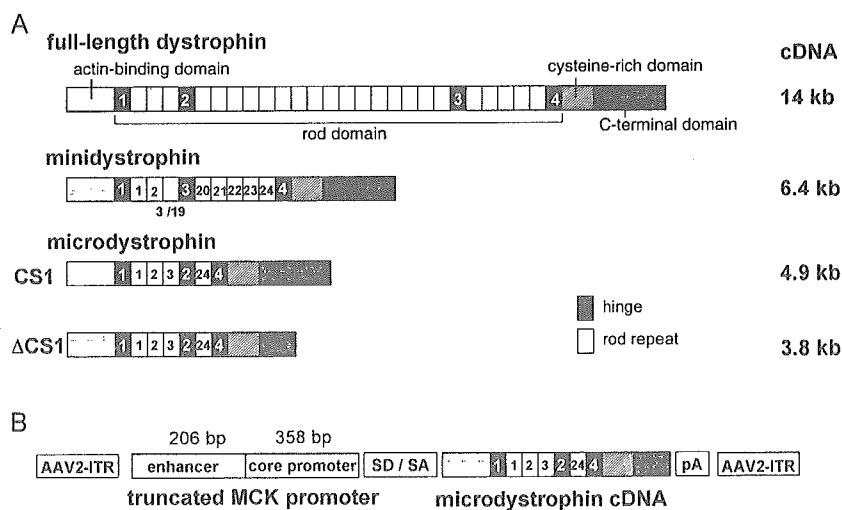
We injected AAV2-MCKΔCS1 into tibialis anterior (TA) muscles of 10-day-old and 5-week-old dystrophin-deficient *mdx* mice ( $7.5 \times 10^{10}$  vector genomes (vg) for neonatal muscle;  $2.5 \times 10^{11}$  vg for young muscle). In a natural course, 10-day-old *mdx* muscle shows no obvious dystrophic changes, while 5-week-old *mdx* muscle shows active cycles of the degeneration–regeneration process. We also analyzed contralateral TA muscles from the treated *mdx* mice and TA muscles from age-matched

C57BL/10 (B10) mice as controls. When examined at 8 and 24 weeks after AAV2-MCKΔCS1 injection, ΔCS1 had correctly localized at the sarcolemma (Figs. 2A and 2C). Western blot using a dystrophin antibody showed a band of the expected size (138 kDa) in the AAV vector-injected *mdx* muscles (Fig. 2G). Most of the ΔCS1-positive fibers were peripherally nucleated when AAV2-MCKΔCS1 was injected into 10-day-old *mdx* muscles (Figs. 2A and 2B). In contrast, we observed both centrally and peripherally nucleated fibers when the vectors were injected into 5-week-old *mdx* muscle (Figs. 2C and 2D). The mean percentages of ΔCS1-positive fibers were  $22.2 \pm 11.4\%$  at 8 weeks and  $16.5 \pm 7.0\%$  at 24 weeks after injection at 10 days of age (Fig. 2E). When injected at 5 weeks of age, the mean percentages of dystrophin-positive fibers were  $39.2 \pm 15.8\%$  at 8 weeks and  $51.5 \pm 17.3\%$  at 24 weeks after vector injection (Fig. 2F). Next, we quantified the amount of ΔCS1 protein by immunoblotting. The amount of microdystrophin protein in the AAV-injected *mdx* muscles at 10 days of age was  $12.7 \pm 8.4\%$  of that of full-length dystrophin in B10 muscle at 8 weeks (data not shown) and  $9.2 \pm 1.4\%$  at 24 weeks after injection (Fig. 2G). When we injected AAV2-MCKΔCS1 into 5-week-old *mdx* muscles, the amount was  $32.6 \pm 8.0\%$  of that of B10 muscle at 8 weeks and  $39.8 \pm 7.0\%$  at 24 weeks after injection (data not shown).

**AAV Vector-Mediated ΔCS1 Expression Ameliorated Dystrophic Phenotypes at 24 Weeks after Injection**

When we analyzed *mdx* muscles treated at 10 days of age at 24 weeks after vector injection, only a small percentage of the ΔCS1-positive fibers ( $12.5 \pm 7.8\%$ ) had central nuclei compared with untreated *mdx* muscle fibers (Fig. 3A), suggesting the protective function of ΔCS1 against muscle degeneration. In contrast, the percentage of

**FIG. 1.** Diagrams of human full-length dystrophin, minidystrophin, and microdystrophin cDNAs (CS1, ΔCS1) and AAV2-MCKΔCS1. (A) Full-length dystrophin has the N-terminal, actin-binding domain, central rod domain with 24 rod repeats and four hinges, cysteine-rich domain, and C-terminal domain. Minidystrophin, which was cloned from a mild Becker patient and reported previously, is shown as a reference [28]. CS1 has the N-terminal domain, a shortened version of the central rod domain with 4 rod repeats and three hinges, the cysteine-rich domain, and the C-terminal domain [14]. To incorporate microdystrophin CS1 cDNA into the AAV2 vector plasmid, we deleted the 3' and 5' untranslated regions and exons 71–78 from CS1 cDNA. The resultant ΔCS1 cDNA is 3.8 kb long. The number of the rod repeats or hinges is shown inside the squares. (B) Structure of the AAV2 vector expressing ΔCS1. ΔCS1 cDNA was incorporated into the AAV2 vector plasmid downstream of the truncated muscle-specific MCK promoter [15].



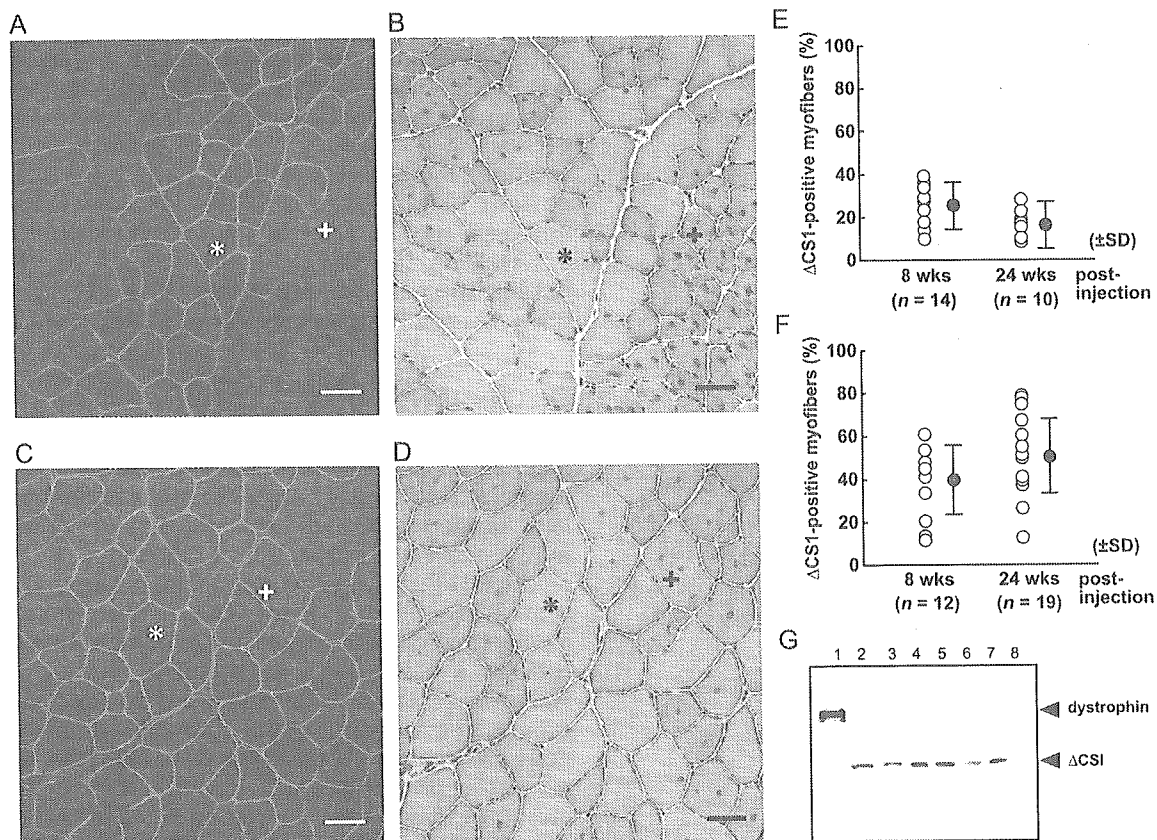


**FIG. 2.**  $\Delta$ CS1 expression after AAV vector-mediated gene transfer into skeletal muscles of dystrophin-deficient *mdx* mice. AAV2-MCK $\Delta$ CS1 was injected into TA muscles of *mdx* mice at (A, B, E) 10 days or at (C, D, F) 5 weeks of age and the muscles were analyzed at 8 or 24 weeks after injection. (A–D) Histological analysis of AAV-injected muscles 24 weeks after AAV injection. Immunofluorescence using a dystrophin antibody (A, C) and H&E staining of serial sections (B, D) is shown.  $\Delta$ CS1 is correctly localized at the sarcolemma (A, C). Most  $\Delta$ CS1-positive fibers (+) showed peripherally located nuclei, and their fiber diameters were relatively larger than  $\Delta$ CS1-negative fibers (+) in the muscles injected at 10 days of age (A, B). In contrast to the muscles injected at the neonatal stage, many centrally nucleated fibers (+) coexist with peripherally nucleated fibers (+) in the muscles injected with the AAV vectors at 5 weeks of age (D). In (A and C), nuclei were stained with TOTO-3 (blue). Bar, 50  $\mu$ m. (E, F) The percentage of  $\Delta$ CS1-positive fibers among all fibers of the injected *mdx* muscle. The means (black circles) are indicated  $\pm$  SD (bars). The percentage of  $\Delta$ CS1-positive fibers in muscles injected at 5 weeks of age (F) was higher than in the muscles injected at 10 days of age (E). (G) Western blot analysis using a dystrophin antibody of AAV-injected *mdx* muscles. Muscles treated at 10 days of age were analyzed at 24 weeks after injection. Lane 1, C57BL/10 muscle; lanes 2–7, AAV vector-injected *mdx* muscles; lane 8, uninjected *mdx* muscle. Full-length dystrophin (lane 1) and  $\Delta$ CS1 (lanes 2–7) were detected at the predicted sizes (427 or 138 kDa, respectively).

centrally nucleated fibers among  $\Delta$ CS1-positive fibers in *mdx* muscles treated at 5 weeks of age ( $51.5 \pm 11.0\%$ ) was higher than that of *mdx* muscles treated at 10 days of age (Fig. 3B).

Next, we evaluated the contractile properties of AAV2-MCK $\Delta$ CS1-injected *mdx* muscle. Untreated *mdx* muscle showed remarkable hypertrophy, but its specific force was much lower than in control B10 muscle (Table 1). Similarly, the wet weight of *mdx* TA muscles treated with AAV2-MCK $\Delta$ CS1 at 10 days of age was much heavier than that of control B10 TA muscles, but importantly, the maximal force was also increased (Table 1). As a result, there was no statistical difference in specific tetanic force between AAV2-MCK $\Delta$ CS1-treated *mdx* muscles and age-matched B10 muscles (Table 1).

The transduction efficiency of AAV2 vector-mediated gene transfer into 10-day-old *mdx* mice was relatively low (only up to 20% of positive fibers) (Fig. 2E) compared to gene transfer into 5-week-old *mdx* mice (around 50%) (Fig. 2F), but, surprisingly, the specific tetanic force at 24 weeks after vector injection was almost equivalent to that of age-matched B10 mice and much higher than that of untreated *mdx* muscle (Table 1). To clarify the mechanism of force generation recovery by small percentages of  $\Delta$ CS1-positive fibers, we next examined the relationship between muscle hypertrophy and force generation. We found a positive correlation ( $r = 0.779$ ,  $P < 0.05$ ) between the wet weight of the AAV2-MCK $\Delta$ CS1-injected TA muscle and the force generation (Fig. 4A), but not between the muscle weight and the relative interstitial

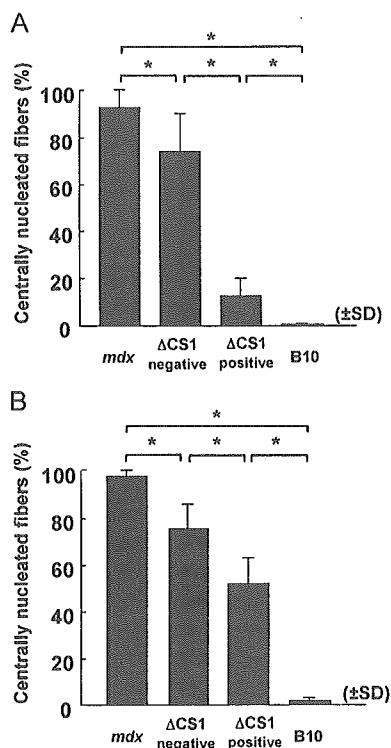


FIG. 3. Microdystrophin  $\Delta$ CS1 prevents muscle degeneration. Quantitative analysis of centrally nucleated fibers among  $\Delta$ CS1-positive and -negative fibers in AAV-injected *mdx* muscle. AAV2-MCK $\Delta$ CS1 was injected into TA muscles of *mdx* mice at (A) 10 days or at (B) 5 weeks of age and analyzed at 24 weeks after injection. Uninjected *mdx* and age-matched control B10 muscles were also examined. (A, B) Most of the  $\Delta$ CS1-positive fibers in muscles injected at 10 days of age have peripherally located nuclei (A). The percentage of centrally nucleated fibers in  $\Delta$ CS1-positive fibers in muscles treated at 5 weeks of age ( $51.5 \pm 11.0\%$ ) (B) was higher than that in muscles treated at 10 days of age ( $12.5 \pm 7.8\%$ ) (A). Note that the ratio of centrally nucleated fibers was significantly reduced even in  $\Delta$ CS1-negative fibers in muscles injected at both ages. \* $P < 0.01$ .

area ( $r = -0.596$ ,  $P > 0.05$ ) (Fig. 4B). To confirm whether increased muscle weight reflected myofiber hypertrophy, we measured individual cross-sectional areas (CSAs) of  $\Delta$ CS1-positive or -negative myofibers in AAV-injected *mdx* muscles. The mean value of fiber CSAs was remarkably larger in  $\Delta$ CS1-positive *mdx* fibers than in B10 fibers (Fig. 4C). Histogram analysis further demonstrated that the fiber CSA distribution of  $\Delta$ CS1-positive *mdx* fibers was shifted to the right compared to that of B10 muscle; larger caliber fibers were dominant, reflecting hypertrophy of  $\Delta$ CS1-expressing fibers (Fig. 4E). Thus, hypertrophied  $\Delta$ CS1-positive fibers seemed to greatly improve contractile force generation. Some of the untreated and  $\Delta$ CS1-negative *mdx* fibers were also hypertrophied, but the hypertrophied fibers seemed not to improve the specific force (Fig. 4E).

When we injected 5-week-old mice, force generation was recovered in AAV-injected *mdx* muscles, as when

we treated 10-day-old mice, but there was no statistically significant difference in muscle weight between AAV-treated *mdx* muscles and B10 muscles (Table 1). The muscle weight had no correlation with the force generation ( $r = -0.512$ ,  $P > 0.05$ ) (data not shown). In addition, hypertrophy of  $\Delta$ CS1-positive fibers was not obvious (Fig. 4D). Therefore, we concluded that improved specific force of the *mdx* muscles treated at 5 weeks of age was achieved without hypertrophy, possibly because approximately 50% of the muscle fibers were fully functional for  $\Delta$ CS1 expression.

## DISCUSSION

The level of dystrophin or minidystrophin expression required for effective gene therapy has not been determined yet, although estimates based on either transgenic *mdx* mouse studies [16–18] or the analysis of asymptomatic carriers of dystrophin-deficiency have been reported [19]. Clerk et al. reported that immunostaining showed very few dystrophin-negative fibers in muscles of asymptomatic DMD carriers, while immunoblot analysis revealed a considerable reduction in dystrophin [19]. Furthermore, it was reported that transgenic *mdx* mice expressing a minidystrophin at only 20–30% of endogenous dystrophin levels showed significantly reduced myopathic phenotypes [17]. Phelps et al. suggested that uniform expression of dystrophin is much more beneficial than the variable pattern when the overall levels of dystrophin expression were the same [18]. These findings suggest that the percentage of dystrophin-expressing fibers is more critical than the total amount of the protein. On the other hand, Rafael et al. showed that the expression of minidystrophin in only half the *mdx* muscle fibers resulted in a markedly milder phenotype than *mdx* mice showed [16], suggesting that dystrophin-positive fibers rescue surrounding dystrophin-negative fibers from degenerative changes. In this study, we administered a recombinant AAV vector containing a human microdystrophin gene to the *mdx* muscle and analyzed the relationship between the level or extent of microdystrophin expression and the recovery of contractile force. Importantly, relatively small percentages of muscle fibers (less than 20%) dramatically improved the specific contractile force of dystrophic muscle. Although the molecular mechanisms by which microdystrophin recovers the specific contractile force remain to be shown, this result is encouraging in that the function of dystrophin-deficient muscle might be greatly improved by fewer dystrophin-positive myofibers than previously estimated. As shown in Fig. 3, however, there is a significant reduction in the percentage of centrally nucleated fibers among  $\Delta$ CS1-negative *mdx* fibers compared to untreated *mdx* muscle, suggesting that microdystrophin expression at levels below the detection limits of immunostaining might be partially protective. There-

TABLE 1: Contractile properties of AAV2-MCK $\Delta$ CS1-injected *mdx* muscle

	Muscle length ( $L_0$ , mm)	Muscle weight (MW, mg)	Maximal force ( $P_0$ , mN)	Specific force <sup>a</sup> (mN/mm <sup>2</sup> )
		Injection at 10 days of age		
B10 ( $n = 4$ )	16.1 $\pm$ 0.9	48.7 $\pm$ 2.8	91.3 $\pm$ 18.1	32.0 $\pm$ 5.9
AAV- <i>mdx</i> ( $n = 7$ )	16.1 $\pm$ 1.2	64.3 $\pm$ 4.7***	116.5 $\pm$ 29.9**	30.9 $\pm$ 7.9**
<i>mdx</i> ( $n = 7$ )	16.1 $\pm$ 1.0	70.9 $\pm$ 7.0*	79.8 $\pm$ 20.0	19.1 $\pm$ 3.8*
		Injection at 5 weeks of age		
B10 ( $n = 6$ )	15.8 $\pm$ 0.9	54.9 $\pm$ 5.7	69.0 $\pm$ 31.0	20.9 $\pm$ 9.0
AAV- <i>mdx</i> ( $n = 11$ )	15.3 $\pm$ 0.8	60.9 $\pm$ 6.8	81.7 $\pm$ 24.2**	22.3 $\pm$ 8.2**
<i>mdx</i> ( $n = 11$ )	15.7 $\pm$ 0.7	67.9 $\pm$ 7.6*	42.2 $\pm$ 26.1	10.9 $\pm$ 7.5*

Force generation was measured 24 weeks after injection. Data are expressed as means  $\pm$  SD.

<sup>a</sup> Specific force = ( $P_0 \times L_0 \times 1.06$ )/MW.

\* Significant difference ( $P < 0.05$ ) compared to B10.

\*\* Significant difference ( $P < 0.05$ ) compared to *mdx* muscles.

fore, exact estimation of the percentage of microdystrophin-positive fibers required for the full amelioration is somewhat difficult.

Recovery of absolute maximal force and specific tetanic force is one of the barometers of amelioration. The difference between the contractile properties of  $\Delta$ CS1-expressing hypertrophied muscle and those of hypertrophied *mdx* muscle by overexpression of IGF-1 [20,21] deserves attention:  $\Delta$ CS1-positive *mdx* muscle showed considerable recovery of specific force, whereas IGF-mediated hypertrophy modestly restored specific force and the muscle remained susceptible to damage. Similarly, a myostatin blockade of treated *mdx* muscle reportedly improved specific force to some extent, but showed a decrease in ECC force to the same extent as control *mdx* muscle [22]. For comparison of the effects of these different approaches toward DMD therapy, the resistance of  $\Delta$ CS1-treated muscle to eccentric contraction remains to be evaluated. Importantly, however, myostatin antibody-treated mice showed significantly decreased serum creatine kinase concentrations, suggesting that myostatin blockade endowed dystrophin-deficient fibers with membrane stability.

Positive correlation between muscle wet weight and specific tetanic force indicates that muscle hypertrophy is responsible for functional amelioration at 10-day-old injected *mdx* mice. However, lack of small-caliber, presumably regenerative fibers is the most prominent finding on histograms of  $\Delta$ CS1-positive *mdx* muscles injected at 10 days of age. Therefore, not only a mild increase in hypertrophic fibers, but also a decrease in small-sized fibers due to inhibition of the cycle of degeneration/regeneration, could greatly contribute to normalization of specific tetanic force. Reduction in embryonic myosin heavy chain and increase in mature myosin heavy chain might contribute to the functional recovery.

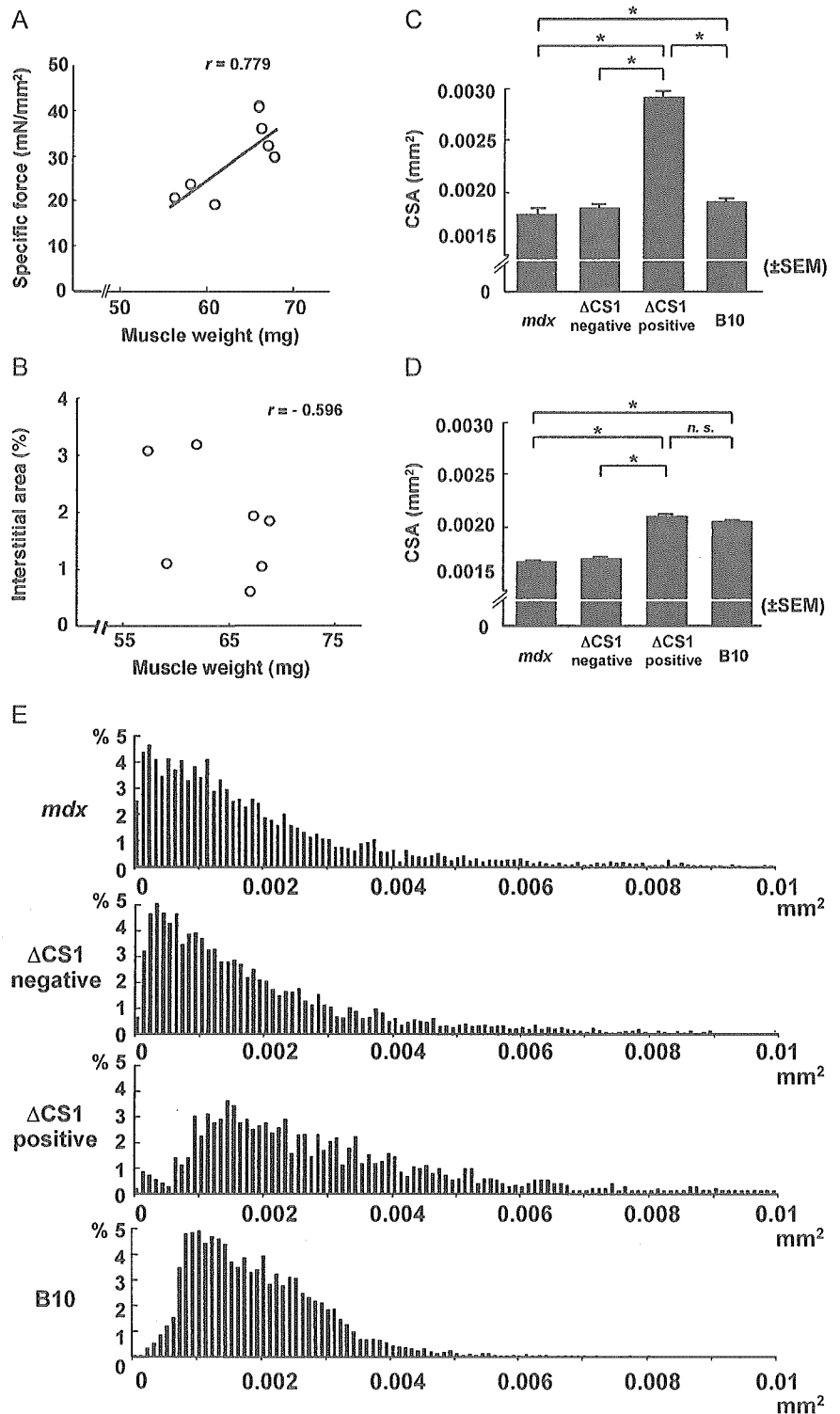
Watchko *et al.* injected an AAV2 vector carrying microdystrophin into *mdx* mice and observed incomplete

recovery of specific tetanic force with 30–60% of dystrophin-positive fibers [13]. Their microdystrophin was slightly longer than our  $\Delta$ CS1, it had three hinges, and the C-terminal domain was also deleted. Subtle differences in the construction could affect the functional aspects, and therefore we think that a functional examination of transgenic *mdx* is inevitable.

We also injected AAV2-MCK $\Delta$ CS1 into 5-week-old *mdx* muscles, which usually show active cycles of muscle degeneration and regeneration. Dystrophin staining revealed that approximately 50% of *mdx* myofibers expressed human-type  $\Delta$ CS1 microdystrophin 24 weeks after injection. There was no obvious sign of an immune response (data not shown). In contrast to neonatal muscle, *mdx* muscles treated at 5 weeks of age were not hypertrophied but still generated improved contractile force, indicating that widely expressed  $\Delta$ CS1 could recover muscle function of adult mice without compensatory hypertrophy. Importantly, the CSAs of  $\Delta$ CS1-positive fibers treated at a neonatal stage were larger than those of  $\Delta$ CS1-positive fibers treated at 5 weeks of age (Figs. 4C and 4D). One possible explanation for this is that neonatal muscle has a high potency of compensatory hypertrophy in response to force deficit.

Our  $\Delta$ CS1 and R4-R23/delta71-78, previously reported by Harper *et al.* [11], have similar structures. R4-R23/delta71-78 robustly transformed centrally nucleated fibers into peripherally nucleated fibers [11]. In contrast, the expression of  $\Delta$ CS1 in adult *mdx* myofibers resulted in a modest reduction of centrally nucleated fibers when introduced into 5-week-old *mdx* muscle (Fig. 3B). A possible explanation for this discrepancy is a difference in the promoters that drive the microdystrophin expression. Harper *et al.* used a muscle-specific, potent promoter, CK6, and the positions of the Kozak sequences or splicing units are different from ours [11]. These differences might greatly influence the timing and levels of microdystrophin expression. A second possible factor

**FIG. 4.**  $\Delta$ CS1-positive *mdx* fibers in AAV-treated muscle at 10 days of age show hypertrophy. TA muscles of *mdx* mice were injected with AAV2-MCK $\Delta$ CS1 at 10 days of age (A–C, E) or at 5 weeks of age (D) and analyzed at 24 weeks after injection. (A) Correlation between muscle wet weight and tetanic force generation ( $n = 7$ ). There was a significant positive correlation between muscle weight and force generation ( $r = 0.779$ ,  $P < 0.01$ ). (B) Relationship between muscle weight and relative interstitial area in AAV-injected muscles ( $n = 7$ ). The increase in muscle weight is not proportional to the interstitial area. (C, D) Mean cross-sectional area (CSA) of uninjected *mdx* muscle fibers and  $\Delta$ CS1-positive or -negative fibers in AAV-injected *mdx* muscles or age-matched B10 muscle fibers. Three TA muscles were examined for each group. The total numbers of fibers traced were 9674, 6347, 1525, and 5877 in (C) and 8077, 4075, 3479, and 5476 in (D) for *mdx*,  $\Delta$ CS1-negative *mdx*,  $\Delta$ CS1-positive *mdx*, and B10 fibers, respectively. When injected at 10 days of age, the CSA of  $\Delta$ CS1-positive *mdx* fibers was definitely larger than that of normal B10,  $\Delta$ CS1-negative *mdx*, or contralateral *mdx* fibers (C). In contrast, when mice were treated at 5 weeks of age, the mean CSA of  $\Delta$ CS1-positive *mdx* fibers was similar to that of B10 muscle and slightly larger than that of *mdx* or  $\Delta$ CS1-negative *mdx* fibers in treated muscle (D). \* $P < 0.01$ . (E) Distribution of the fiber CSAs of untreated *mdx*,  $\Delta$ CS1-positive, or  $\Delta$ CS1-negative fibers in *mdx* muscles injected at 10 days of age and age-matched B10 fibers. Shown are the same data set presented in (C). In untreated *mdx* muscles or in  $\Delta$ CS1-negative *mdx* fibers, small-caliber fibers are dominant, reflecting regeneration. The distribution pattern of  $\Delta$ CS1-positive fibers deviated to the right, reflecting a larger size than that of B10 fibers. Similar to B10 muscles, small-caliber fibers were markedly reduced in  $\Delta$ CS1-positive *mdx* fibers, indicating that  $\Delta$ CS1 prevented muscle degeneration.



is the difference in muscle types used. Harper *et al.* injected AAV vectors into gastrocnemius muscles of 32-day-old mice. The gastrocnemius shows less centrally

nucleated fibers than TA muscle in the natural course of the disease (Yuasa *et al.*, unpublished data). In our result, however, AAV-treated *mdx* muscle with a high

percentage of centrally nucleated fibers (50%) did not show dystrophic dysfunction, e.g., decreased force generation. Therefore, centrally nucleated fibers do not disprove the protective function of  $\Delta$ CS1. The percentage of centrally nucleated fibers would reflect the state of muscles at the time of injection. Our results are important because it is sometimes difficult to start gene therapies before the onset of the clinical course of DMD, and AAV2-MCK $\Delta$ CS1 is expected to show therapeutic effects even after the onset of disease.

Although we injected high titers of AAV-vector particles into the muscle, the transduction efficiency in 10-day-old *mdx* muscles was much lower than that in 5-week-old *mdx* muscle. This phenomenon was also noticed for the injection of AAV2-CMVlacZ into neonatal B10 muscle (unpublished results). This difference might be due to the preferential expression of receptors or coreceptors for an AAV-2 particle on adult muscle fibers. Several molecules, such as heparan sulfate proteoglycan [23],  $\alpha$ v $\beta$ 5 integrin [24], and dynamin I [25], are proposed to play certain roles in AAV type 2 infection, although the expression of these molecules in muscle fibers during development and aging has not been fully determined. Another possibility is dilution of AAV vectors by rapid growth of neonatal muscle. When we cultured satellite cells prepared from AAV2-CMVlacZ-injected *mdx* muscle, we observed no blue myoblasts or myotubes (data not shown). Therefore, proliferation and fusion of nontransduced satellite cells/myoblasts would greatly dilute the microdystrophin protein.

Our results are promising because AAV vector-mediated  $\Delta$ CS1 gene transfer had a restorative function for dystrophin-deficient *mdx* muscle. However, demonstration of the benefits of this gene transfer strategy for human DMD patients requires careful testing. Differences between humans and mice, such as muscle size, life span, or biological properties (especially immune responses), should be taken into consideration. A bigger animal model, e.g., canine X-linked muscular dystrophy [26], will contribute to the preclinical study of gene therapy.

## MATERIALS AND METHODS

**Constructs of human rod-truncated microdystrophin cDNAs and generation of AAV vectors expressing microdystrophin.** To incorporate microdystrophin CS1 cDNA (4.9 kb) [14] into an AAV type 2 vector, we further deleted the 3' and 5' UTRs and exons 71–78 from CS1 cDNA. In brief, DNA fragments of the 5'-terminal and 3'-terminal regions were independently amplified by PCR to remove exons 71–78 and the 5' and the 3' UTRs and then replace them with corresponding sequences of CS1 cDNA. The resulting microdystrophin cDNA was 3.8 kb long and designated  $\Delta$ CS1. Microdystrophin  $\Delta$ CS1 cDNA was then cloned into an AAV type 2 vector plasmid [15]. The recombinant AAV vector expressing  $\Delta$ CS1 under the control of the truncated muscle-specific MCK promoter, designated AAV2-MCK $\Delta$ CS1, was then purified and titrated as previously described [15].

**Administration of AAV vector to murine skeletal muscle.** Fifteen microliters ( $7.5 \times 10^{10}$  vg) or 50  $\mu$ l ( $2.5 \times 10^{11}$  vg) of AAV2-MCK $\Delta$ CS1 was injected directly into the right TA muscles of dystrophin-deficient C57BL/10 *mdx* mice at 10 days or 5 weeks of age, respectively. AAV vector-injected and uninjected *mdx* muscles and normal muscles of age-matched C57BL/10 mice were isolated at 8 and 24 weeks after injection.

**Contractile properties of AAV2-MCK $\Delta$ CS1-injected TA muscles.** Tetanic force generation was measured and analyzed as described previously with some modifications [14,27]. The entire TA muscle was removed with its tibial origin intact, and the distal portion of the TA tendon and its origin was secured with a 5-0 silk suture. The TA was mounted in a vertical tissue chamber and connected to a force transducer, UL-10GR (Minerva, Nagano, Japan), and a length servosystem, MM-3 (Narishige, Tokyo, Japan). Electrical stimulation using a SEN3301 (Nihon Kohden, Tokyo, Japan) was applied through a pair of platinum wires placed on both sides of the muscle in physiological soft solution (150 mM NaCl, 4 mM KCl, 2 mM CaCl<sub>2</sub>, 1 mM MgCl<sub>2</sub>, 5.6 mM glucose, 5 mM Hepes, pH 7.4, and 0.02 mM D-tubocurarine). Muscle fiber length was adjusted incrementally by using a micropositioner until peak isometric twitch force responses were obtained (optimal fiber length ( $L_0$ )). Maximal tetanic force ( $P_0$ ) was assessed by stimulation frequencies of 125 pulses/s delivered in 500-ms duration trains with 2 min intervening between each train. Following two measurements, the stimulated muscle was weighed after tendon and bone attachments were removed. All forces were normalized to the physiological cross-sectional area (pCSA), the latter estimated on the basis of the following formula: muscle wet weight (in mg)/( $L_0$  (in mm)  $\times$  1.06 (in mg/mm<sup>3</sup>)). The estimated pCSA was used to determine specific tetanic force ( $P_0$ /pCSA) of the muscle. After measurement of contractile force, the muscle was quickly frozen in liquid nitrogen-cooled isopentane for histopathological analysis.

**Histopathological analyses.** Histological, immunohistochemical, and Western blot analyses were performed as described [14]. After blocking with an M.O.M. kit (Vector Laboratories, Burlingame, CA, USA), dystrophin was detected using a monoclonal anti-dystrophin antibody NCL-DysB (Novocastra, Newcastle, UK; 1:20 dilution) and visualized with Alexa 488-labeled goat anti-mouse IgG antibody (Molecular Probes, Eugene, OR, USA) (1:200 dilution). Nuclei were stained with TOTO-3 (Molecular Probes). In some cases, the signal was visualized with diaminobenzidine and counterstained with hematoxylin. We counted the number of centrally or peripherally nucleated fibers in dystrophin-positive or -negative fibers of whole cross sections of TA muscle. In addition, the CSA of each fiber was measured using an image analysis system, ImagePro-Plus (Media Cybernetics, Silver Spring, MD, USA). To evaluate the level of fibrosis, we performed modified Masson trichrome staining, and the blue-stained area was measured using Image Pro-Plus. The relative connective tissue area was calculated to the entire muscle cross-sectional area (%). The signals on immunoblotting were quantitated using NIH Image.

**Statistical analysis.** Data were expressed as means  $\pm$  SD or  $\pm$  SEM. If a significant *F* ratio was detected by analysis of variance, comparisons among each group were performed using Fisher's PLSD. A *P* value of <0.05 or <0.01 was considered statistically significant. The relation between the muscle weight and the specific tetanic force was analyzed with Pearson's correlation coefficient (*P* < 0.05).

## ACKNOWLEDGMENTS

We are greatly appreciative of Ryoko Nakagawa and Satoru Masuda for their technical support. We thank Ayako Sakamoto, Kunimasa Arima (Department of Laboratory Medicine, National Center Hospital for Mental, Nervous and Muscular Disorders), and Michiko Sagishima (Department of Pathology, School of Medicine, Teikyo University) for advising on pathological techniques. This work is supported by Grants-in-Aid from the Center of Excellence, Research on Nervous and Mental Disorders (10B-1, 13B-1), and Health Sciences Research Grants for Research on the Human Genome and Gene Therapy (H10-genome-015, H13-genome-001) from the Ministry of Health, Labor, and Welfare of

Japan, and a Grant-in-Aid for Scientific Research (B) from the Ministry of Education, Science, Sports, and Culture of Japan.

RECEIVED FOR PUBLICATION FEBRUARY 28, 2004; ACCEPTED JULY 20, 2004.

## REFERENCES

- Acsadi, G., et al. (1991). Human dystrophin expression in *mdx* mice after intramuscular injection of DNA constructs. *Nature* 29: 815–818.
- Gilbert, R., et al. (2001). Dystrophin expression in muscle following gene transfer with a fully deleted ("guttled") adenovirus is markedly improved by trans-acting adenoviral gene products. *Hum. Gene Ther.* 20: 1741–1755.
- DelloRusso, C., et al. (2002). Functional correction of adult *mdx* mouse muscle using gutted adenoviral vectors expressing full-length dystrophin. *Proc. Natl. Acad. Sci. USA* 99: 12979–12984.
- Lu, Q. L., et al. (2003). Functional amounts of dystrophin produced by skipping the mutated exon in the *mdx* dystrophic mouse. *Nat. Med.* 9: 1009–1014.
- Bartlett, R. J., et al. (2000). In vivo targeted repair of a point mutation in the canine dystrophin gene by a chimeric RNA/DNA oligonucleotide. *Nat. Biotechnol.* 18: 615–622.
- Xiao, X., Li, J., and Samulski, R. J. (1996). Efficient long-term gene transfer into muscle tissue of immunocompetent mice by adeno-associated virus vector. *J. Virol.* 70: 8098–8108.
- Kessler, P. D., et al. (1996). Gene delivery to skeletal muscle results in sustained expression and systemic delivery of a therapeutic protein. *Proc. Natl. Acad. Sci. USA* 26: 14082–14087.
- Fisher, K. J., et al. (1997). Recombinant adeno-associated virus for muscle directed gene therapy. *Nat. Med.* 3: 306–312.
- Yuasa, K., et al. (1998). Effective restoration of dystrophin-associated proteins in vivo by adenovirus-mediated transfer of truncated dystrophin cDNAs. *FEBS Lett.* 27: 329–336.
- Wang, B., Li, J., and Xiao, X. (2000). Adeno-associated virus vector carrying human minidystrophin genes effectively ameliorates muscular dystrophy in *mdx* mouse model. *Proc. Natl. Acad. Sci. USA* 5: 13714–13719.
- Harper, S. Q., et al. (2002). Modular flexibility of dystrophin: implications for gene therapy of Duchenne muscular dystrophy. *Nat. Med.* 8: 253–261.
- Fabb, S. A., Wells, D. J., Serpente, P., and Dickson, G. (2002). Adeno-associated virus vector gene transfer and sarcolemmal expression of a 144 kDa micro-dystrophin effectively restores the dystrophin-associated protein complex and inhibits myofibre degeneration in nude/*mdx* mice. *Hum. Mol. Genet.* 1: 733–741.
- Watchko, J., et al. (2002). Adeno-associated virus vector-mediated minidystrophin gene therapy improves dystrophic muscle contractile function in *mdx* mice. *Hum. Gene Ther.* 10: 1451–1460.
- Sakamoto, M., et al. (2002). Micro-dystrophin cDNA ameliorates dystrophic phenotypes when introduced into *mdx* mice as a transgene. *Biochem. Biophys. Res. Commun.* 17: 1265–1272.
- Yuasa, K., et al. (2002). Adeno-associated virus vector-mediated gene transfer into dystrophin-deficient skeletal muscles evokes enhanced immune response against the transgene product. *Gene Ther.* 9: 1576–1588.
- Rafael, J., et al. (1994). Prevention of dystrophic pathology in *mdx* mice by a truncated dystrophin isoform. *Hum. Mol. Genet.* 3: 1725–1733.
- Wells, D., et al. (1995). Expression of human full-length and minidystrophin in transgenic *mdx* mice: implications for gene therapy of Duchenne muscular dystrophy. *Hum. Mol. Genet.* 4: 1245–1250.
- Phelps, S. F., et al. (1995). Expression of full-length and truncated dystrophin minigenes in transgenic *mdx* mice. *Hum. Mol. Genet.* 4: 1251–1258.
- Clerk, A., et al. (1991). Characterisation of dystrophin in carriers of Duchenne muscular dystrophy. *J. Neurol. Sci.* 102: 197–205.
- Gregorevic, P., Plant, D. R., Leeding, K. S., Bach, L. A., and Lynch, G. S. (2002). Improved contractile function of the *mdx* dystrophic mouse diaphragm muscle after insulin-like growth factor-I administration. *Am. J. Pathol.* 161: 2263–2272.
- Barton, E. R., Morris, L., Musaro, A., Rosenthal, N., and Sweeney, H. L. (2002). Muscle-specific expression of insulin-like growth factor I counters muscle decline in *mdx* mice. *J. Cell Biol.* 157: 137–148.
- Bogdanovich, S., et al. (2002). Functional improvement of dystrophic muscle by myostatin blockade. *Nature* 28: 418–421.
- Summerford, C., and Samulski, R. J. (1998). Membrane-associated heparan sulfate proteoglycan is a receptor for adeno-associated virus type 2 virions. *J. Virol.* 72: 1438–1445.
- Summerford, C., Bartlett, J. S., and Samulski, R. J. (1999). AlphaVbeta5 integrin: a coreceptor for adeno-associated virus type 2 infection. *Nat. Med.* 5: 78–82.
- Duan, D., et al. (1999). Dynamin is required for recombinant adeno-associated virus type 2 infection. *J. Virol.* 73: 10371–10376.
- Shimatsu, Y., et al. (2003). Canine X-linked muscular dystrophy in Japan (CXMDj). *Exp. Anim.* 52: 93–97.
- Hosaka, Y., et al. (2002). Alpha1-syntrophin-deficient skeletal muscle exhibits hypertrophy and aberrant formation of neuromuscular junctions during regeneration. *J. Cell Biol.* 16: 1097–1107.
- England, S. B., et al. (1990). Very mild muscular dystrophy associated with the deletion of 46% of dystrophin. *Nature* 343: 180–182.



## Mac-1<sup>low</sup> early myeloid cells in the bone marrow-derived SP fraction migrate into injured skeletal muscle and participate in muscle regeneration ☆

Koichi Ojima<sup>a,b</sup>, Akiyoshi Uezumi<sup>a</sup>, Hiroyuki Miyoshi<sup>c</sup>, Satoru Masuda<sup>a</sup>,  
Yohei Morita<sup>d,e</sup>, Akiko Fukase<sup>a</sup>, Akihito Hattori<sup>b</sup>, Hiromitsu Nakauchi<sup>d,e</sup>,  
Yuko Miyagoe-Suzuki<sup>a</sup>, Shin'ichi Takeda<sup>a,\*</sup>

<sup>a</sup> Department of Molecular Therapy, National Institute of Neuroscience, National Center of Neurology and Psychiatry, 4-1-1 Ogawa-higashi, Kodaira, Tokyo 187-8502, Japan

<sup>b</sup> Department of Animal Science, Faculty of Agriculture, Hokkaido University, Kita 9, Nishi 9, Kita-ku, Sapporo, Hokkaido 060-8589, Japan

<sup>c</sup> BioResource Center, RIKEN Tsukuba Institute, 3-1-1 Koyadai, Tsukuba, Ibaraki 305-0074, Japan

<sup>d</sup> Laboratory of Stem Cell Therapy, Center for Experimental Medicine, The Institute of Medical Science, The University of Tokyo, 4-6-1 Shirokanedai, Minato-ku, Tokyo 108-8639, Japan

<sup>e</sup> Department of Immunology, Institute of Basic Medical Sciences, The University of Tsukuba, and CREST (JST), 1-1-1 Tennodai, Tsukuba, Ibaraki 305-8575, Japan

Received 20 May 2004

### Abstract

Recent studies have shown that bone marrow (BM) cells, including the BM side population (BM-SP) cells that enrich hematopoietic stem cells (HSCs), are incorporated into skeletal muscle during regeneration, but it is not clear how and what kinds of BM cells contribute to muscle fiber regeneration. We found that a large number of SP cells migrated from BM to muscles following injury in BM-transplanted mice. These BM-derived SP cells in regenerating muscles expressed different surface markers from those of HSCs and could not reconstitute the mouse blood system. BM-derived SP/Mac-1<sup>low</sup> cells increased in number in regenerating muscles following injury. Importantly, our co-culture studies with activated satellite cells revealed that this fraction carried significant potential for myogenic differentiation. By contrast, mature inflammatory (Mac-1<sup>high</sup>) cells showed negligible myogenic activities. Further, these BM-derived SP/Mac-1<sup>low</sup> cells gave rise to mononucleate myocytes, indicating that their myogenesis was not caused by stochastic fusion with host myogenic cells, although they required cell-to-cell contact with myogenic cells for muscle differentiation. Taken together, our data suggest that neither HSCs nor mature inflammatory cells, but Mac-1<sup>low</sup> early myeloid cells in the BM-derived SP fraction, play an important role in regenerating skeletal muscles.

© 2004 Elsevier Inc. All rights reserved.

**Keywords:** Side population cells; Muscle regeneration; Myogenic differentiation; Bone marrow; Muscular dystrophy

☆ **Abbreviations:**  $\beta$ -Gal,  $\beta$ -galactosidase; BM, bone marrow; CTX, cardiotoxin; FACS, fluorescence-activated cell sorting; GC, gastrocnemius; GFP, green fluorescence protein; HE, hematoxylin and eosin; HSC, hematopoietic stem cell; MP, main population; SP, side population; TA, tibialis anterior; X-Gal, 5-bromo-4-chloro-3-indolyl  $\beta$ -D-galactopyranoside.

\* Corresponding author. Fax: +81 42 346 1750.

E-mail address: [takeda@ncnp.go.jp](mailto:takeda@ncnp.go.jp) (S. Takeda).

Skeletal muscles have a remarkable capacity for regeneration in response to various types of damage, such as chemicals, stretching, exercise, injury, and diseases including inherited muscular dystrophies. Satellite cells are skeletal muscle-specific precursors and play an important role in muscle fiber regeneration [3]. They are located beneath the basement membrane and are mitotically

quiescent in adult muscle. Once muscle is damaged, they are activated, proliferate enormously, and fuse with each other or with pre-existing muscle fibers to produce fully mature muscle fibers [3,33]. They have been considered the only cells that give rise to myoblasts and form new myofibers in adult skeletal muscle [3,38].

Recently, cells with myogenic potential have been found in non-muscle tissues. They are involved in bone marrow (BM) [4–6,8,12,13,15,18,22,35], dorsal aorta [10], fetal liver [15], synovial membrane [11], and epidermis [24]. Among them, BM is an attractive source tissue for cell-based therapy for muscular dystrophy because it is thought that BM cells with myogenic potential are disseminated to all muscles in the body through the circulation. More recently, LaBarge and Blau [22] demonstrated that transplanted BM cells were progressively recruited as satellite cells and that subsequent exercise induced them to participate in muscle regeneration, suggesting that donor-derived BM cells contribute to muscle fibers in a step-wise biological progression.

Furthermore, it has been reported that BM side population (BM-SP) cells, which efficiently efflux Hoechst dye 33342 and enrich hematopoietic stem cells (HSCs) [16,17], participated in skeletal muscle regeneration in lethally irradiated mice [7,18]. Recently, Camargo et al. [6] and Corbel et al. [8] have reported that a single BM-SP cell was able to both reconstitute the hematopoietic system and contribute to muscle regeneration. Although Camargo et al. [6] suggested that cells committed to the myeloid lineage were incorporated into newly forming myofibers, it is still unclear what types of myeloid cells preferentially contribute to regenerating myofibers.

Several BM transplantation studies [4,6,8,12,15,18,22] indicate that donor-derived myofibers are frequently detected in regenerated fibers or in exercised muscles, although they are quite rare in normal conditions. This phenomenon is possibly related to increased recruitment of BM-derived myogenic progenitor cells or stem cells into damaged muscle via the blood stream. In addition, it is likely that cytokines released in inflamed muscles direct the myogenic commitment of BM cells.

Here we demonstrated that a large number of SP cells migrated from BM to regenerating muscles, where the BM-derived SP cells did not have hematopoietic potential but did directly participate in muscle regeneration. Further, we showed that cells with myogenic potential were enriched in BM-derived SP cells with low expression of Mac-1 antigen in regenerating muscles. These findings further support the potential of BM-SP cell-based therapy for dystrophic muscular disorders.

## Materials and methods

*Experimental animals.* All procedures used on experimental animals were approved by the Experimental Animal Care and Use Committee

at the National Institute of Neuroscience. C57BL/6 mice were purchased from Nihon CLEA (Tokyo, Japan). C57BL/6-*GFP*-transgenic mice were kindly provided by Dr. Okabe (Osaka University, Japan). C57BL/6-Rosa26 mice were obtained from the Jackson Laboratory (Bar Harbor, ME).

*Preparation of BM and BM-SP cells.* Bone marrow cells were sterilely isolated from the femurs and tibias of *GFP* transgenic mice [27]. Marrow fragments were filtered through 40  $\mu$ m nitrex mesh (BD Bioscience, Franklin Lakes, NJ) and subsequently through 10  $\mu$ m nylon mesh (Kyoshin Rikoh, Tokyo, Japan). After removing red blood cells with Lympholyte-M (Cedarlane, Hornby, Ontario), BM cells were used for BM cell-transplantation or isolation of SP cells.

The BM-SP fraction was prepared as described by Goodell et al. (<http://www.bcm.tmc.edu/genetherapy/goodell/newsite/protocols.html>). BM cells were re-suspended at  $10^6$  cells/ml in Dulbecco's modified Eagle's medium (DMEM) (Invitrogen, Carlsbad, CA) containing 2% fetal bovine serum (FBS) (Trace Biosciences, New South Wales, Australia), 10 mM HEPES, and 5  $\mu$ g/ml Hoechst 33342 (Sigma Chemical, St. Louis, MO) and incubated for 90 min at 37°C in the presence or the absence of 50  $\mu$ M Verapamil (Sigma). For antibody staining, cells were incubated on ice for 30 min in the presence of a 1:100 dilution of PE- or APC-conjugated anti-CD45 antibody, PE-conjugated anti-CD11b/CD18 (Mac-1) antibody, PE-conjugated Sca-1 antibody, biotin-conjugated anti-CD34 antibody, or biotin-conjugated anti-c-kit antibody (BD PharMingen, San Diego, CA). For biotin-conjugated antibodies, 1:100 diluted PE- or APC-conjugated streptavidin (BD PharMingen) was further labeled for 15 min on ice. After washing, stained cells were re-suspended in PBS containing 2% FBS and 2  $\mu$ g/ml propidium iodide (PI) (BD PharMingen). Cell sorting was performed on a FACS VantageSE flow cytometer (Falcon, Franklin Lakes, NJ). Hoechst staining and subsequent antibody labeling indicated a viability of  $84.2 \pm 11.5\%$  (means  $\pm$  SD,  $n = 18$ ) as expressed by the percentage of total PI-negative cells per total cells. The BM-SP accounted for  $0.026 \pm 0.017\%$  (means  $\pm$  SD,  $n = 18$ ) of viable unfractionated BM without red blood cells. Debris and dead cells were excluded by forward scatter, side scatter, and PI gating. We used only PI-negative fractions for further experiments.

*Preparation of mononucleated cells from muscle.* Cardiotoxin (CTX) (Wako Pure Chemical Industries, Tokyo, Japan)-injected and uninjected skeletal muscles were dissected from *GFP*<sup>+</sup>BM-SP/CD45<sup>+</sup> cell-transplanted mice and the *GFP* transgenic mice. We carefully removed nerves, blood vessels, tendons, and fat tissues from muscles under a dissection microscope. Trimmed muscles were minced and then treated with 0.2% type II collagenase (Worthington Biochemical, Lakewood, NJ) for 40 min at 37°C [20]. Muscle slurries were filtered through 100  $\mu$ m nitrex mesh (BD Bioscience) and subsequently through 40  $\mu$ m nitrex mesh (BD Bioscience). Erythrocytes were eliminated by treatment with 0.8% NH<sub>4</sub>Cl in Tris-buffer solution. Mononucleated cells were stained with Hoechst 33342 and antibodies as described in BM-SP staining. Then stained cells were analyzed with a FACS VantageSE flow cytometer (Falcon). Hoechst staining and subsequent antibody labeling indicated a viability of  $87.5 \pm 1.3\%$  (means  $\pm$  SD,  $n = 3$ ) and  $68.5 \pm 3.2\%$  (means  $\pm$  SD,  $n = 3$ ) expressed as the percentage of total PI-negative cells per total mononucleated cells from injured muscles and uninjured muscles, respectively. The SP cells accounted for  $0.81 \pm 0.25\%$  (means  $\pm$  SD,  $n = 9$ ) and  $1.72 \pm 0.13\%$  (means  $\pm$  SD,  $n = 3$ ) of viable unfractionated mononucleate cells without red blood cells from injured muscles and uninjured muscles, respectively. We used only PI-negative fractions for further experiments.

*Transplantation experiments.* After X-irradiation with 5 or 9 Gy (Hitachi Medical, Tokyo, Japan),  $5 \times 10^6$ – $1 \times 10^7$  unfractionated *GFP*<sup>+</sup> BM cells, 2000 *GFP*<sup>+</sup> BM-SP/CD45<sup>+</sup> cells, or 3000 *GFP*<sup>+</sup> SP/CD45<sup>+</sup> cells from regenerating muscles of *GFP* transgenic mice were transplanted retroorbitally into 8- to 10-week-old C57BL/6 mice. For transplantation of *GFP*<sup>+</sup> SP/CD45<sup>+</sup> cells from BM and *GFP*<sup>+</sup> SP/CD45<sup>+</sup> cells from regenerating muscles,  $2 \times 10^5$  unfractionated BM cells from C57BL/6 mice were also transplanted as competitor cells. SP

cells were isolated from PI-negative fractions and immediately used for transplantation assay. GFP chimerism was calculated by the ratio of GFP<sup>+</sup> cells to total mononucleated cells in BM or peripheral blood. Twelve to 15 weeks after transplantation, transplanted mice were subjected to CTX injection studies and FACS analysis.

**Cardiotoxin injection and tissue preparation.** To induce muscle regeneration, 0.1 ml of 10  $\mu$ M CTX was injected into the TA and/or GC muscles of transplanted mice with a 27-gauge needle [9,14,19]. The CTX-injected TA and/or GC muscles and the non-injected contralateral TA and/or GC muscles were dissected for histological analysis at 3–4 weeks or 8–10 weeks after CTX injection. Following fixation with 4% paraformaldehyde in PBS for 30 min, muscles were sequentially soaked in 10% sucrose in PBS and 20% sucrose in PBS. For histological and immunohistochemical analysis, muscles were frozen in isopentane cooled with liquid nitrogen.

**Histological and immunohistochemical analysis.** Muscle cryostat sections (7  $\mu$ m) were stained with hematoxylin and eosin (HE). Serial cross-sections were blocked with 5% goat serum in PBS and then reacted with anti-GFP antibody (1:100; Chemicon International, Temecula, CA), anti-laminin  $\alpha$ 2 antibody (1:100; clone 4H8-2; Alexis, San Diego, CA), anti-CD11b/18 (Mac-1) antibody (1:100; Cedarlane), and/or anti-M-cadherin antibody (1:10,000) at 4°C overnight. Anti-M-cadherin antibody was generated by fusing the mouse M-cadherin cDNA sequence corresponding to 339–444 aa to GST in a pGEX vector (Amersham Biosciences, Piscataway, NJ), and the GST-M-cadherin fusion protein was used as an antigen. The rabbit anti-serum obtained was affinity purified. The sections were incubated with appropriate combinations of Alexa 488-, Alexa 568-, and Alexa 594-labeled secondary antibodies (Molecular Probes, Eugene, OR) for 30 min. Nuclei were stained with TOTO3 (Molecular Probes). Stained sections were observed under a confocal laser scanning microscope (Leica TCS SP; Leica, Heidelberg, Germany).

**Preparation of activated satellite cells.** Single myofibers were prepared as described in the literature [2,31] with slight modifications. In brief, dissected extensor digitorum longus (EDL) muscles from C57BL/6 mice or C57BL/6-Rosa26 mice were digested with 0.5% type I collagenase (Worthington Biochemical) at 37°C for 90 min. Five to ten intact, viable single myofibers were plated on chamber slides (Nalge Nunc International, Naperville, IL) coated with Matrigel (Collaborative Biomedical Products, Bedford, MA), and cultured with DMEM (Invitrogen) containing 10% horse serum (HS) (BioWhittaker, Walkersville, MD) and 0.5% chick embryo extract (CEE) (Invitrogen) in a humid 5% CO<sub>2</sub> environment at 37°C for 4 days. To proliferate mononucleated myogenic cells, they were kept in growth medium (10% HS, 20% FBS, and 1% CEE in DMEM).

For immunostaining, cultured cells were fixed with 2% formaldehyde in PBS for 10 min. After washing with 0.5% Triton X-100 in PBS, specimens were blocked with 5% goat serum (Cedarlane) in PBS for 15 min, then incubated with anti-GFP antibody (1:500; Chemicon) and anti-sarcomeric  $\alpha$ -actinin antibody (1:1000; Sigma) for 1 h at 37°C, and then reacted with secondary antibody conjugated with Alexa 488 or Alexa 568 (Molecular Probes). Nuclei were detected with Hoechst 33258 (Molecular Probes). To detect  $\beta$ -galactosidase activity, cells were stained with 5-bromo-4-chloro-3-indolyl  $\beta$ -D-galactopyranoside (X-Gal).

**Co-culture of BM-derived SP cells with activated satellite cells.** After approximately 7 days culture, myofiber-derived activated satellite cells reached 50–70% confluence. At this point, co-culture with BM-SP cells was started. Approximately 500–2500 freshly isolated GFP<sup>+</sup> BM-SP/CD45<sup>+</sup> cells were added to 3000–5000 activated satellite cells derived from C57BL/6 myofibers. Differentiation medium (10% HS, 2% FBS, and 0.5% CEE in DMEM) was applied soon after starting co-culture. Approximately 4000–5000 SP/CD45<sup>+</sup> cells, 4000–5000 SP/CD45<sup>+</sup> Mac-1<sup>-</sup> cells, 2000 SP/CD45<sup>+</sup> Mac-1<sup>low</sup> cells, 10,000 main population (MP)/CD45<sup>+</sup> cells, 10,000 MP/CD45<sup>+</sup> Mac-1<sup>low</sup> cells, or 10,000 MP/CD45<sup>+</sup> Mac-1<sup>+</sup> cells from GFP transgenic mouse muscles damaged by CTX injection were co-cultured with 10,000 activated satellite cells from C57BL/6 mice. For BM-derived SP cells from regenerating

muscles, cells were kept in growth medium (20% FBS, 2.5 ng/ml basic fibroblast growth factor (Pepro Tech EC, London, England) in DMEM) for 4 days and then switched to differentiation medium for further culture. Less than 20% of plated BM-SP cells survived 2 days after starting co-culture. Approximately 5–10% plated BM-derived cells from regenerating muscles survived 2 days after starting co-culture. Cultured cells were observed with phase-contrast and fluorescence microscopy IX70 (OLYMPUS, Tokyo, Japan).

## Results

### Contribution of BM-SP cells to muscle fibers in vivo

To investigate which type of donor cells contributes to muscle fibers, unfractionated BM cells or BM-SP cells from GFP transgenic mice [27] were transplanted into X-irradiated C57BL/6 mice. To further compare the efficiency of myogenic contributions of donor-derived cells to damaged muscles or intact muscles, we injected cardiotoxin (CTX) into tibialis anterior (TA) and/or gastrocnemius (GC) muscles more than 12 weeks after transplantations to induce muscle regeneration. For BM-SP cell transplantation, we selected the CD45<sup>+</sup> fraction of BM-SP cells (BM-SP/CD45<sup>+</sup>) to exclude the possible contamination of mesenchymal stem cells [34]. The frequency of donor-derived GFP<sup>+</sup> fibers in damaged muscle was relatively higher than in undamaged muscle (Fig. 1, Table 1). The ratio of GFP<sup>+</sup> myofibers normalized to the number of transplanted cells was significantly higher in BM-SP/CD45<sup>+</sup> cell-transplanted mice than in unfractionated BM cell-transplanted mice (Table 1). Contrary to previous reports [15,22], we have not detected donor-derived GFP<sup>+</sup> satellite cells in muscle sections and in cultures of isolated single myofibers from transplanted mice (data not shown).

### Migration of SP cells from BM to regenerating muscle

CTX injection experiments suggested that muscle damage enhanced the contribution of BM-SP/CD45<sup>+</sup> cells to muscle fiber formation and that muscle injuries could increase the migration of BM cells with myogenic potential to the injury site via the bloodstream. Therefore, we examined whether SP cells migrate or not from BM to regenerating muscle by the use of GFP<sup>+</sup> BM-SP/CD45<sup>+</sup> cell-transplanted mice. Twelve to 15 weeks after transplantation, CTX was injected into TA muscles. Three days after the injury, a considerable number of donor-derived GFP<sup>+</sup> cells were found in damaged muscles (Figs. 2A–D). At this early stage of muscle regeneration, M-cadherin immunostaining revealed many activated satellite cells proliferating inside the pre-existing basement membrane sheath (Fig. 2E).

Next, we isolated mononucleated cells from intact or damaged muscles and analyzed them by fluorescence-activated cell sorting (FACS). SP cells, which are sensitive to Verapamil, were involved in both intact and damaged

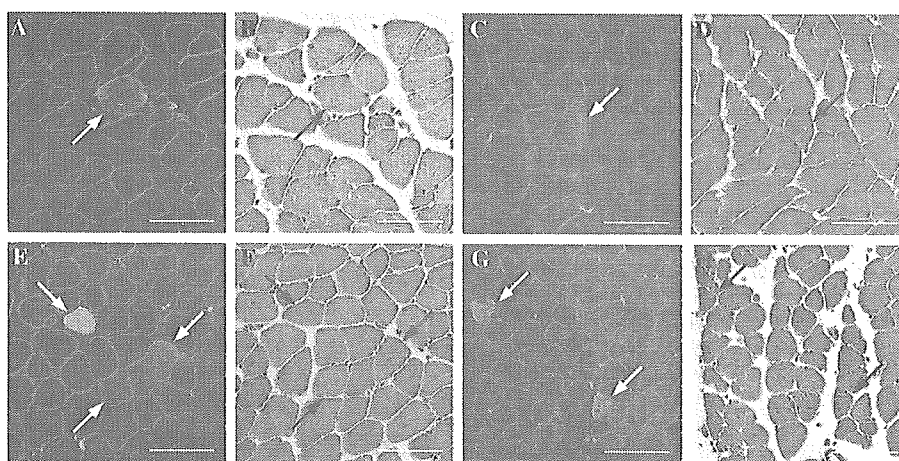


Fig. 1. Contribution of transplanted BM cells to myofibers in mice. (A–H) Unfractionated GFP<sup>+</sup> BM cells (A,B,E, and F) or GFP<sup>+</sup> BM-SP/CD45<sup>+</sup> cells (C,D,G, and H) were transplanted into lethally X-irradiated C57BL/6 mice. Twelve to 15 weeks after transplantation, CTX was injected into TA and/or GC muscles to induce muscle regeneration (E–H). Undamaged muscles are shown in (A–D). At 10 weeks after CTX injection, cryostat sections of TA (A,B,E,F,G, and H) and GC (C,D) muscles were stained with anti-GFP antibody (green in A,C,E, and G) and anti-laminin  $\alpha$ 2 antibody (red in A,C,E, and G). HE-stained sections (B,D,F, and H) are serial sections of (A,C,E, and G), respectively. Arrows indicate GFP-positive myofibers. Bars, 80  $\mu$ m.

Table 1  
Quantitation of donor-derived myofibers in transplanted mice

Mouse ID No.	X-ray (Gy)	Transplanted cell	GFP-chimerism in BM (%)	Muscle	CTX <sup>a</sup>	GFP <sup>+</sup> myofibers	Total myofibers	% <sup>b</sup>	% <sup>c</sup>
52	9	GFP <sup>+</sup> BM	73.4	TA	4w	2	1368	0.15	0.0002
				GC	4w	18	3234	0.56	0.0018
				TA	—	0	2120	0.00	0.0000
				GC	—	4	3505	0.11	0.0004
4	5	GFP <sup>+</sup> BM	43.4	TA	8w	5	1581	0.32	0.0005
				GC	8w	24	3093	0.78	0.0024
				TA	—	2	1304	0.15	0.0002
				GC	—	0	4658	0.00	0.0000
14	5	GFP <sup>+</sup> BM	46.7	TA	10w	13	1564	0.83	0.0013
				GC	10w	44	1378	3.19	0.0044
				TA	—	0	1150	0.00	0.0000
				GC	—	1	2634	0.04	0.0001
73	9	GFP <sup>+</sup> BM	77.7	TA	10w	1	1044	0.10	0.0002
				GC	10w	0	3171	0.00	0.0000
				TA	—	0	1138	0.00	0.0000
				GC	—	0	556	0.00	0.0000
84	9	GFP <sup>+</sup> BM-SP/CD45 <sup>+</sup>	42.7	TA	3w	2	1205	0.17	0.1000
				TA	—	0	1189	0.00	0.0000
106	9	GFP <sup>+</sup> BM-SP/CD45 <sup>+</sup>	22.9	TA	3w	3	767	0.39	0.1500
				TA	—	0	773	0.00	0.0000
61	9	GFP <sup>+</sup> BM-SP/CD45 <sup>+</sup>	92.9	TA	10w	18	735	2.45	0.7965
				GC	10w	12	1176	1.02	0.5310
				TA	—	0	584	0.00	0.0000
				GC	—	4	2071	0.19	0.1770
69	9	GFP <sup>+</sup> BM-SP/CD45 <sup>+</sup>	10.4	TA	10w	0	405	0.00	0.0000
				GC	10w	7	2838	0.25	0.3500
				TA	—	0	1024	0.00	0.0000
				GC	—	1	2889	0.03	0.0500

<sup>a</sup> CTX was injected more than 12 weeks after transplantation. Mice were sacrificed 3, 4, 8, or 10 weeks after CTX injection.

<sup>b</sup> % = (the number of GFP<sup>+</sup> myofibers/the total number of myofibers per muscle section)  $\times$  100.

<sup>c</sup> % = (the number of GFP<sup>+</sup> myofibers/the number of transplanted cells)  $\times$  100.

muscles (Figs. 2F–G and I–J). To characterize SP cells in muscles, they were further fractionated by CD45 and GFP expression. GFP<sup>+</sup> SP/CD45<sup>+</sup> cells significantly

increased in number in injured muscles, when compared with uninjured muscles (Figs. 2H and K). In both uninjured and injured muscles, GFP<sup>+</sup> SP cells were

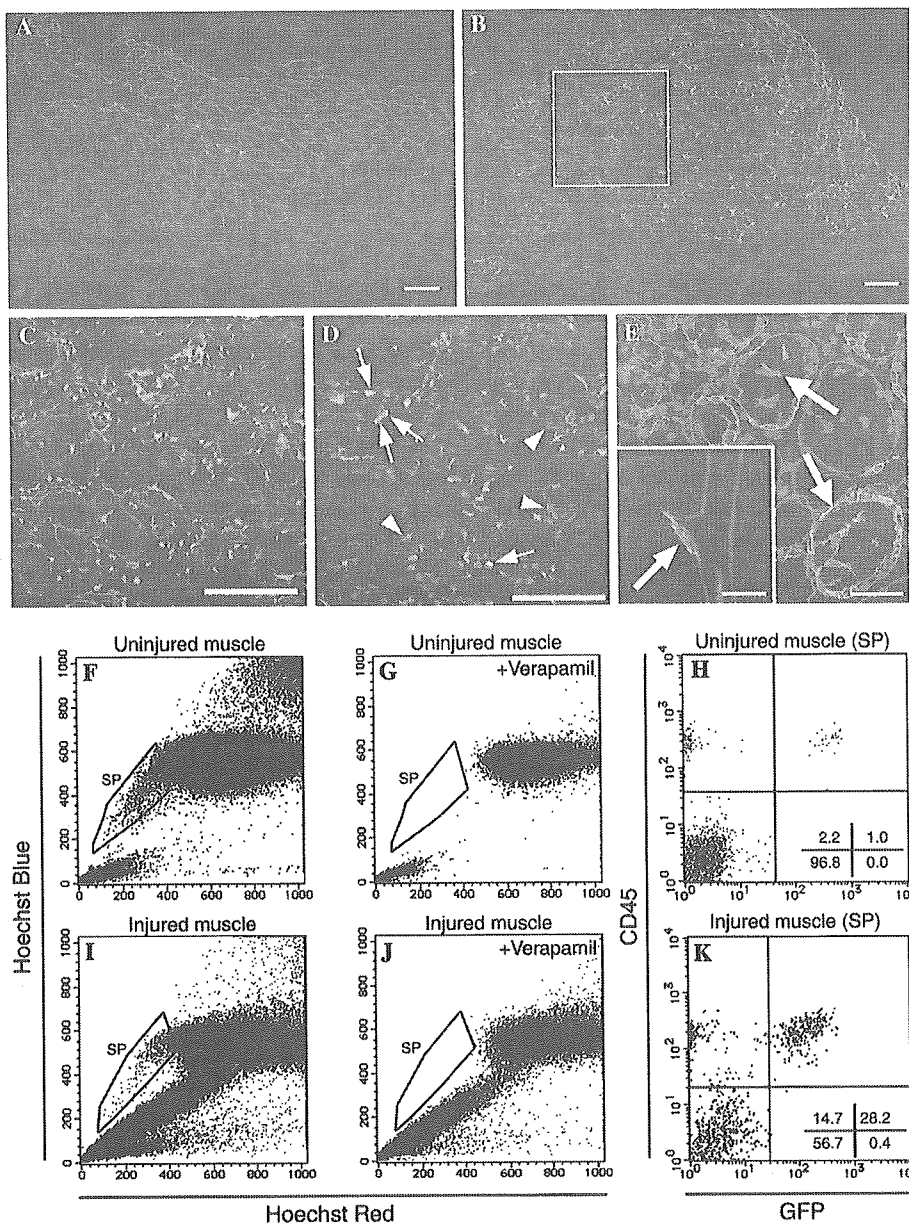


Fig. 2. Migration of BM-derived SP cells to regenerating skeletal muscle. (A,B) Immunofluorescent staining for GFP (green) and laminin  $\alpha 2$  (red) of TA muscle cross-cryosections from GFP<sup>+</sup> BM-SP/CD45<sup>+</sup> cell-transplanted mice. (A) Only a few GFP<sup>+</sup> mononucleated cells were observed in intact muscle. (B) In contrast to (A), a great number of GFP<sup>+</sup> mononucleated cells have infiltrated into damaged muscle at 3 days after CTX injection. (C) A high magnification photograph of the inset area of (B), displaying triple immunofluorescent staining for GFP (green), laminin  $\alpha 2$  (red), and nuclei (blue). GFP<sup>+</sup> cells were located in intra- and extra-basement membranes. (D) At 3 days after CTX injection, a cryostat section of regenerating muscle of a mouse transplanted with GFP<sup>+</sup> BM-SP/CD45<sup>+</sup> cells was stained with anti-Mac-1 antibody (red) and anti-GFP antibody (green). Nuclei were stained with TOTO3 (blue). Arrows indicate both GFP<sup>+</sup> and Mac-1<sup>+</sup> positive cells. Arrowheads indicate GFP<sup>+</sup> but Mac-1<sup>-</sup> cells. (E) A cryostat section of regenerating muscle at day 3 after CTX injection was stained with anti-M-cadherin antibody (green) and anti-laminin  $\alpha 2$  antibody (red). Nuclei were stained with TOTO3 (blue). Arrows indicate M-cadherin<sup>+</sup> activated satellite cells. Our anti-M-cadherin antibody specifically recognized a satellite cell beneath the basement membrane in control muscle (arrow in inset of E). (F–K) Representative FACS analyses demonstrating that mononucleated cells isolated from uninjured muscles (F–H) or regenerating muscles (I–K) of GFP<sup>+</sup> BM-SP/CD45<sup>+</sup> cell-transplanted mice contained Verapamil-sensitive SP cells. These SP cells were further characterized with GFP and CD45 expression (H,K). Note that the percentage of a subfraction of SP cells expressing both GFP and CD45 was considerably increased at 3 days after CTX injection. In contrast, BM-derived SP cells expressing GFP but not CD45 were hardly detected in both regenerating and undamaged muscles. BM-GFP chimerisms of transplanted mice shown here were 93% (F–H) and 60% (I–K), respectively. Three uninjured mice and nine injured mice were analyzed and showed a similar tendency (data not shown). Bars, 100  $\mu$ m in (A–D), 40  $\mu$ m in (E), and 8  $\mu$ m in inset of (E).

largely CD45<sup>+</sup> (Figs. 2H and K). Moreover, in GFP<sup>+</sup> BM-transplanted mice with more than 95% chimerism, nearly 100% of GFP<sup>+</sup> cells were CD45<sup>+</sup> (Uezumi

et al., unpublished data), in agreement with previous reports [6,21,23]. We, therefore, selected CD45<sup>+</sup> cells to pursue the fate of BM-derived cells after muscle injury.

Table 2  
GFP-chimerism in peripheral blood of transplanted mice

Number of transplanted mice	Transplanted cell <sup>a</sup>	Number of transplanted cells	GFP-chimerism in PB (%) <sup>b</sup>
3	GFP <sup>+</sup> SP/CD45 <sup>+</sup>	3000	0.09–0.32

<sup>a</sup> Transplanted cells were prepared from CTX-injected muscles (day 3) of *GFP* transgenic mice.

<sup>b</sup> GFP-chimerism in peripheral blood (PB) was determined at 4 weeks after transplantation.

#### *Failure of BM-derived SP cells isolated from regenerating muscles to reconstitute the blood system of recipient mice*

We observed that a large number of SP cells migrated from BM to muscles following injury. To directly examine whether migrated BM-derived SP cells in regenerating muscles had hematopoietic ability or not, we transplanted 3000 freshly isolated BM-derived SP/CD45<sup>+</sup> cells from regenerating muscles of *GFP* transgenic mice into lethally irradiated recipient mice ( $n = 3$ ). Less than 1% of the peripheral blood cells of recipient mice were donor-derived GFP<sup>+</sup> blood cells 4 weeks after transplantation (Table 2), indicating that BM-derived SP cells in regenerating muscle contained very few or no hematopoietic stem and/or progenitor cells.

#### *Analysis of surface marker expression on BM-derived SP cells*

Previous studies showed that BM-SP cells and BM-derived SP cells in uninjured muscles possess hematopoietic potential [16–18,20]. However, our transplant studies suggested that BM-derived SP/CD45<sup>+</sup> cells in regenerating muscles were different from HSCs even if they had the SP phenotype. To compare the surface marker expression, we isolated three different SP cells, BM-SP cells, BM-derived SP cells of uninjured muscles, and BM-derived SP cells of injured muscles. They were labeled with antibodies to CD45 and one of the following markers: Sca-1, c-kit, CD34, or Mac-1 (Fig. 3A). We detected all markers on BM-SP cells, and their expression levels were similar to previous reports [16–18,28]. We observed a small percentage of c-kit<sup>+</sup> cells in the BM-derived uninjured muscle SP cells (Fig. 3A). However, importantly there were no c-kit<sup>+</sup> BM-derived SP cells in injured muscles (Fig. 3A).

Interestingly, BM-derived SP cells contained Mac-1<sup>low</sup> cells in both injured and uninjured muscles (Figs. 3A, C, and E). These BM-derived SP/CD45<sup>+</sup> Mac-1<sup>low</sup> cells in day 3 CTX-injected muscles increased in numbers (by muscle weight) approximately 18-fold, compared with uninjured muscles. We found that BM-derived SP/Mac-1<sup>low</sup> cells were not labeled with anti-F4/80 antibody, which is a specific and sensitive marker for mature mouse macrophages (data not shown). In contrast, BM-derived Mac-1<sup>high</sup> cells were fallen into the MP fraction (Figs. 3B–E) and expressed

F4/80 antigen (data not shown). These results suggest that SP/CD45<sup>+</sup> Mac-1<sup>low</sup> cells actively migrated from BM to injured muscles and that they were not mature myeloid cells.

#### *Myogenic differentiation of BM-SP cells and BM-derived SP cells isolated from regenerating muscle*

To analyze the cellular mechanism of myogenic differentiation of BM-SP cells and BM-derived SP cells from regenerating muscles in vitro, we first co-cultured BM-SP/CD45<sup>+</sup> cells from *GFP* transgenic mice with activated satellite cells of C57BL/6 mice. We found that GFP<sup>+</sup> BM-SP cells formed multinucleated myotubes (Fig. 4A). These myotubes expressed desmin and sometimes spontaneously contracted (data not shown). To determine whether BM-SP/CD45<sup>+</sup> cells fuse with host myogenic cells or not, we co-cultured BM-SP/CD45<sup>+</sup> cells prepared from *GFP* transgenic mice with activated satellite cells derived from Rosa26 mice, which express  $\beta$ -galactosidase ( $\beta$ -Gal) under a ubiquitous regulatory element [37]. X-gal staining showed that GFP<sup>+</sup> myotubes expressed  $\beta$ -Gal, indicating that BM-SP cells fused with co-cultured host myogenic cells and formed heterokaryotic myotubes (Figs. 4B and C). When GFP<sup>+</sup> BM-SP/CD45<sup>+</sup> cells were cultured alone in the differentiation medium or in the conditioned medium prepared from myogenic cells, they did not form GFP<sup>+</sup> myotubes (data not shown), suggesting that BM-SP/CD45<sup>+</sup> cells formed myotubes via cell-to-cell contact with myogenic cells.

Next, we examined whether migrated BM-derived SP cells isolated from regenerating muscles differentiated into skeletal muscle cells in vitro or not. We focused on Mac-1 expression of BM-derived SP cells because the results, shown in Fig. 3, indicated that considerably greater number of BM-derived Mac-1<sup>low</sup> SP cells infiltrated into injured muscles than into uninjured muscles. In addition, it has been recently reported that monocytes differentiate into various cell types in certain culture conditions [39]. We fractionated BM-derived cells prepared from *GFP* transgenic mouse muscles damaged by CTX injection based on both Mac-1 expression and SP phenotype: SP/CD45<sup>+</sup> cells, SP/CD45<sup>+</sup> Mac-1<sup>-</sup> cells, SP/CD45<sup>+</sup> Mac-1<sup>low</sup> cells, MP/CD45<sup>+</sup> cells, MP/CD45<sup>+</sup> Mac-1<sup>low</sup> cells, and MP/CD45<sup>+</sup> Mac-1<sup>high</sup> cells. Then each fraction was co-cultured with activated satellite cells from C57BL/6 mice. After 14 days of co-culture, they were fixed and stained with anti-GFP antibody

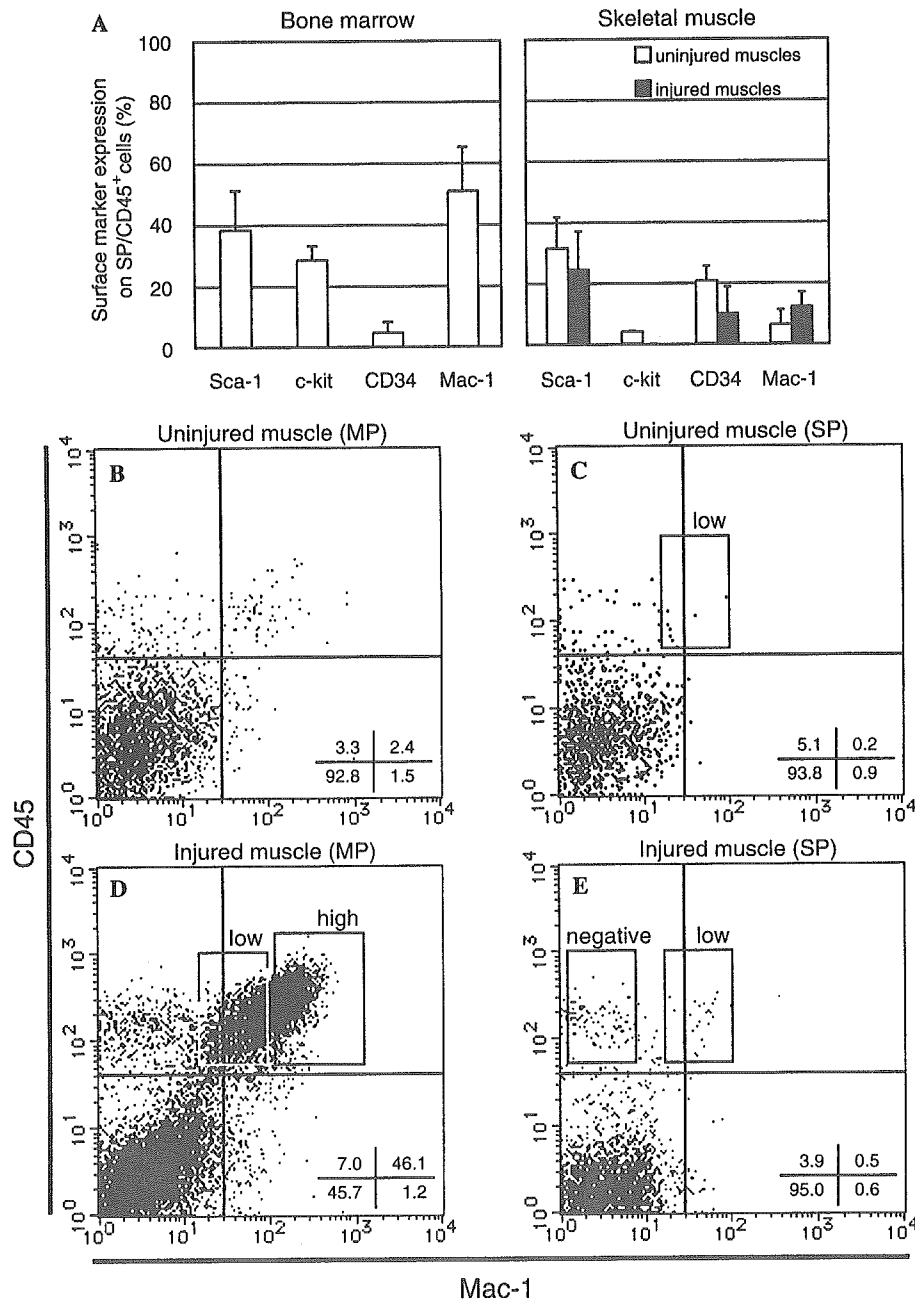


Fig. 3. Analysis of surface marker expression on BM-derived SP/CD45<sup>+</sup> cells prepared from muscles. (A) SP cells from BM (left graph), BM-derived SP cells from uninjured (white columns in right graph), and BM-derived SP cells from injured muscles (black columns in right graph) were isolated and then stained with anti-CD45 antibody and one of the following markers: Sca-1, c-kit, CD34, or Mac-1. The percentages of surface marker expression on BM-SP/CD45<sup>+</sup> cells (left graph) and on BM-derived SP/CD45<sup>+</sup> cells (right graph) were calculated by the following formula: (%) = 100 × (the number of surface marker-positive CD45<sup>+</sup> cells in the SP fraction)/(the number of CD45<sup>+</sup> cells in the SP fraction). Note that the expression of c-kit in BM-derived SP/CD45<sup>+</sup> cells from injured muscles was not at a detectable level. All values (means ± SD) are based on at least three separate experiments. (B–E) Representative FACS analysis demonstrating that mononucleated cells in the MP fraction (B,D) or the SP fraction (C,E) isolated from uninjured muscles (B,C) or injured muscles (D,E) of the GFP transgenic mice. In injured muscles, MP/CD45<sup>+</sup> cells expressed Mac-1 with a broad range of intensities (D). By contrast, the SP fraction from injured muscles contained not CD45<sup>+</sup> Mac-1<sup>high</sup> cells but CD45<sup>+</sup> Mac-1<sup>low</sup> cells (E). Importantly this SP/CD45<sup>+</sup> Mac-1<sup>low</sup> fraction increased in cell number as well as in ratio after muscle injury (rectangles marked “low” in C,E; also see A). The SP sub-fractions shown by rectangles in (D,E) were isolated and then used in further culture experiments (see Fig. 4 and Table 3).

and anti-sarcomeric  $\alpha$ -actinin antibody (Figs. 4D–F). BM-derived SP cells gave rise to myotubes more effectively than BM-derived MP cells (Table 3). In particular, the BM-derived SP/CD45<sup>+</sup> Mac-1<sup>low</sup> fraction was highly

concentrated in cells capable of myotube formation (Table 3). More importantly, sarcomeric  $\alpha$ -actinin-expressing mononucleate myocytes were observed in our co-culture system (Figs. 4G–J), indicating that

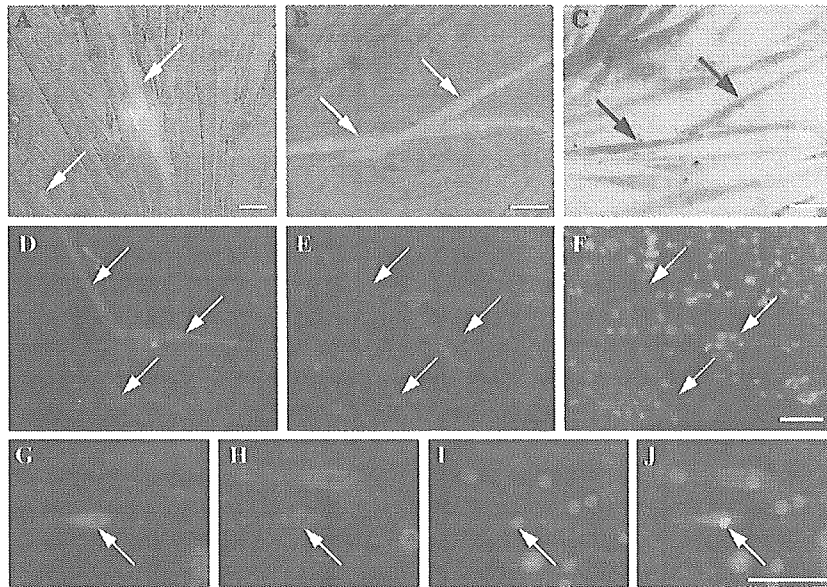


Fig. 4. Myogenic differentiation of BM-SP/CD45<sup>+</sup> cells and BM-derived SP/CD45<sup>+</sup> Mac-1<sup>low</sup> cells from regenerating muscles. (A) GFP<sup>+</sup> BM-SP/CD45<sup>+</sup> cells isolated from GFP transgenic mice were co-cultured with activated satellite cells from C57BL/6 mice. GFP<sup>+</sup> multinucleated myotubes (arrows) were observed after 14 days of co-culture. (B,C) GFP<sup>+</sup> BM-SP/CD45<sup>+</sup> cells were co-cultured with activated satellite cells prepared from ROSA26 mice. (B) A representative image of living GFP<sup>+</sup> myotubes at 21 days co-culture. (C) After fixation, cells were counterstained with X-gal. Arrows show heterokaryotic myotubes expressing both GFP and  $\beta$ -galactosidase. (D–J) Co-culture of GFP<sup>+</sup> BM-derived SP/CD45<sup>+</sup> cells from injured muscles of GFP transgenic mice with activated satellite cells from C57BL/6. Immunofluorescent staining for GFP (D,G and green in F,J), sarcomeric  $\alpha$ -actinin (E,H and red in F,J), and Hoechst 33258 (I, blue in F,J) at 14 days co-culture of BM-derived SP/CD45<sup>+</sup> Mac-1<sup>low</sup> cells (a rectangle indicates “low” in Fig. 3E) from regenerating muscles of the GFP transgenic mice with activated satellite cells of C57BL/6 mice. (D–F) Arrows indicate GFP<sup>+</sup> multinucleated myotubes expressing sarcomeric  $\alpha$ -actinin. (G–J) Arrows indicate a GFP<sup>+</sup> mononucleated cell expressing sarcomeric  $\alpha$ -actinin. Note that a mononucleated cell derived from the GFP<sup>+</sup> SP/CD45<sup>+</sup> Mac-1<sup>low</sup> fraction differentiated into a myogenic cell before fusion with host muscle cells (arrows). Bars, 50  $\mu$ m.

Table 3  
Frequency of GFP<sup>+</sup> myotube formation in co-culture with activated satellite cells

Cultured cells		No. of experiments	No. of cells seeded	No. of GFP <sup>+</sup> myotubes	Frequency of GFP <sup>+</sup> myotubes (%) <sup>a</sup>
Tissue	Cell type				
Regenerating muscle	SP/CD45 <sup>+</sup>	2	21,500	51	0.24
	SP/CD45 <sup>+</sup> Mac-1 <sup>-</sup>	3	23,000	65	0.28
	SP/CD45 <sup>+</sup> Mac-1 <sup>low</sup>	3	6600	34	0.52
	MP/CD45 <sup>+</sup>	2	20,000	4	0.02
	MP/CD45 <sup>+</sup> Mac-1 <sup>low</sup>	3	62,700	44	0.07
	MP/CD45 <sup>+</sup> Mac-1 <sup>high</sup>	3	70,500	19	0.03

<sup>a</sup> % = (the number of GFP<sup>+</sup> myotubes/the number of seeded cells)  $\times$  100.

BM-derived SP/CD45<sup>+</sup> Mac-1<sup>low</sup> cells from regenerating muscles had the ability to differentiate into skeletal muscle cells and did not simply fuse with host myogenic cells to form heterokaryotic myotubes. Although BM-derived MP/CD45<sup>+</sup> Mac-1<sup>high</sup> cells formed myotubes at low frequency, we have not observed mononucleated myocytes from MP/CD45<sup>+</sup> Mac-1<sup>high</sup> cells in our co-culture system. We next injected BM-derived SP/CD45<sup>+</sup> Mac-1<sup>low</sup> cells from regenerating muscles into TA muscles of NOD-scid mice, and we detected a few GFP-positive fibers (not shown).

## Discussion

### Contribution of BM cells to muscle fiber regeneration

The number of donor-derived muscle fibers normalized to the number of transplanted cells was significantly higher in BM-SP/CD45<sup>+</sup> cell-transplanted mice than in unfractionated BM cell-transplanted mice. These results suggest that cells with myogenic potential are enriched in the BM-SP/CD45<sup>+</sup> cell fraction. We and other groups [6,8,12,13,15,18,22] have observed that muscle damage

increased the frequency of donor-derived myofibers in mice. Thus, muscle damage and subsequent regeneration could be important for the participation of donor-derived cells in skeletal muscle regeneration and, in particular, for recruitment of BM cells to damaged muscle.

#### *Migration of SP cells from BM to regenerating muscles*

We showed, for the first time, that a considerable number of SP cells migrated from BM to regenerating muscle together with inflammatory cells such as monocytes/macrophages at the early stage of muscle regeneration. The release of a variety of cytokines/chemokines into regenerating muscle [19] suggests that certain kinds of chemotactic factors, which have an analogous mechanism to monocytes/macrophages, recruit BM-SP cells to regenerating muscles. At this stage of muscle regeneration, satellite cells are activated and proliferate enormously to form fully matured multinucleated cells [3]. Hence, regenerating muscles could provide opportunities for BM-derived SP cells to come into contact with myogenic cells.

#### *Absence of hematopoietic stem and/or progenitor cells in the BM-derived SP fraction isolated from regenerating muscles*

One of the most interesting aspects of BM-derived SP cells in regenerating muscles is the lack of hematopoietic potential. It has been reported that BM-SP cells were able to reconstitute the hematopoietic system in lethally irradiated mice [16,17]. In fact, in our transplantation, 2000 BM-SP/CD45<sup>+</sup> cells reconstituted the hematopoietic system in mice. Likewise, at least 137 uninjured muscle-derived SP/CD45<sup>+</sup> cells have been reported to reconstitute the mouse blood system [23]. However, 3000 SP/CD45<sup>+</sup> cells isolated from regenerating muscles in this study failed to reconstitute the blood system in recipients. Uninjured muscles contained c-kit<sup>+</sup> BM-derived SP cells (our results [23]), even if the level of c-kit expression detectable was low. BM-derived SP cells from injured muscles did not express c-kit antigen, although c-kit is one of the key surface markers for hematopoietic stem and/or hematopoietic progenitor cells [26]. Therefore, our results suggest that BM-derived SP cells in regenerating muscles contain neither HSCs nor hematopoietic progenitors.

#### *Early myeloid cells in the BM-derived SP fraction of regenerating muscles*

Scharenberg et al. [32] have reported that BM-SP cells sharply down-regulated *ABCG2* at the stage of lineage commitment, resulting in loss of the SP phenotype. In fact, our surface marker analysis revealed that BM-derived SP cells from regenerating muscles did not

contain either Mac-1<sup>high</sup> or F4/80<sup>+</sup> cells, which are mature inflammatory cells, but did contain Mac-1<sup>low</sup> cells. In addition, it has been reported that early myeloid cells expressed a low level of Mac-1 antigen [1,29,30]. Therefore, the BM-derived SP fraction should contain early myeloid cells rather than mature inflammatory cells. Our results showed that these early myeloid (BM-derived SP/CD45<sup>+</sup> Mac-1<sup>low</sup>) cells were considerably mobilized to muscles after injury.

#### *Enrichment of cells with myogenic differentiation in BM-derived SP/CD45<sup>+</sup> Mac-1<sup>low</sup> cells*

Camargo et al. [6] demonstrated that myeloid intermediates were incorporated into myofiber formation in response to injury using the lysozyme-M/Cre transgene tracing strategy. More recently, it was shown that the expression of lysozyme-M does not specifically mark cells with myeloid commitment but marks all kinds of hematopoietic cells in their transgene tracing strategy [36]. Hence, it remained unclear what types of cell fractions in BM-derived cells were incorporated into myotubes/myofibers. Here, our co-culture studies clearly revealed that isolated BM-derived SP/CD45<sup>+</sup> Mac-1<sup>low</sup> fraction prepared from regenerating muscles showed the highest myogenic differentiation ability among several BM-derived fractions. In addition, BM-derived cells abruptly lost their myogenic differentiation efficiency after they lost the SP phenotype, suggesting that the myotube formation efficiency of BM-derived cells from regenerating muscles was dependent on their maturation stage.

Zhao et al. [39] have shown that monocytes in peripheral blood differentiated into various cell types under their specific differentiation conditions. In addition, BM-derived myogenic progenitors transiently expressed the low level of Mac-1 antigen at the early process of muscle differentiation [25]. Their results together with ours suggest that BM-derived early myeloid cells might convert to other cell lineages including the myogenic cell lineage in certain circumstances, such as regenerating muscles. Our direct transplantation of muscle-derived Mac-1<sup>low</sup> SP cells from GFP transgenic mice into TA muscles of NOD-scid mice, however, resulted in low efficient GFP-positive myotube formation (data not shown). Although a considerable number of injected cells die shortly after the injection due to innate immune response by the host, the results, together with in vitro co-culture experiments (GFP-positive myotube formation rate: ave. 0.52%), indicate that the efficiency of myogenic conversion of Mac-1<sup>low</sup> SP cells is relatively low, compared with muscle satellite cells.

#### *Myogenic differentiation mechanism of SP cells*

Our co-culture studies revealed that BM-derived SP cells as well as BM-SP cells formed myotubes with host

myogenic cells. Importantly, we found skeletal muscle-specific protein expressing mononucleate myocytes that originated from BM-derived SP/CD45<sup>+</sup> Mac-1<sup>low</sup> cells in regenerating muscles. This result strongly suggests that BM-derived SP cells commit to the myogenic cell lineage before fusion with host myogenic cells and that this myogenic contribution is not a random but a step-wise progressive event. A subset of SP cells would adjust to a new environment and start a myogenic differentiation program. Probably its trigger is cell-to-cell contact between SP cells and myogenic cells rather than soluble

factors, because conditioned medium of cultured myogenic cells had no effect on myogenic differentiation of SP cells in vitro (data not shown). In addition, we have not observed myotubes in cultures of SP cells alone (data not shown).

Taken together, our results revealed that early myeloid cells in the BM-derived SP fraction are implicated in skeletal muscle regeneration in the presence of pre-existing myogenic cells. In our proposed model (Fig. 5), a large number of BM-derived SP cells migrate to regenerating muscles in response to injury. These mobilized

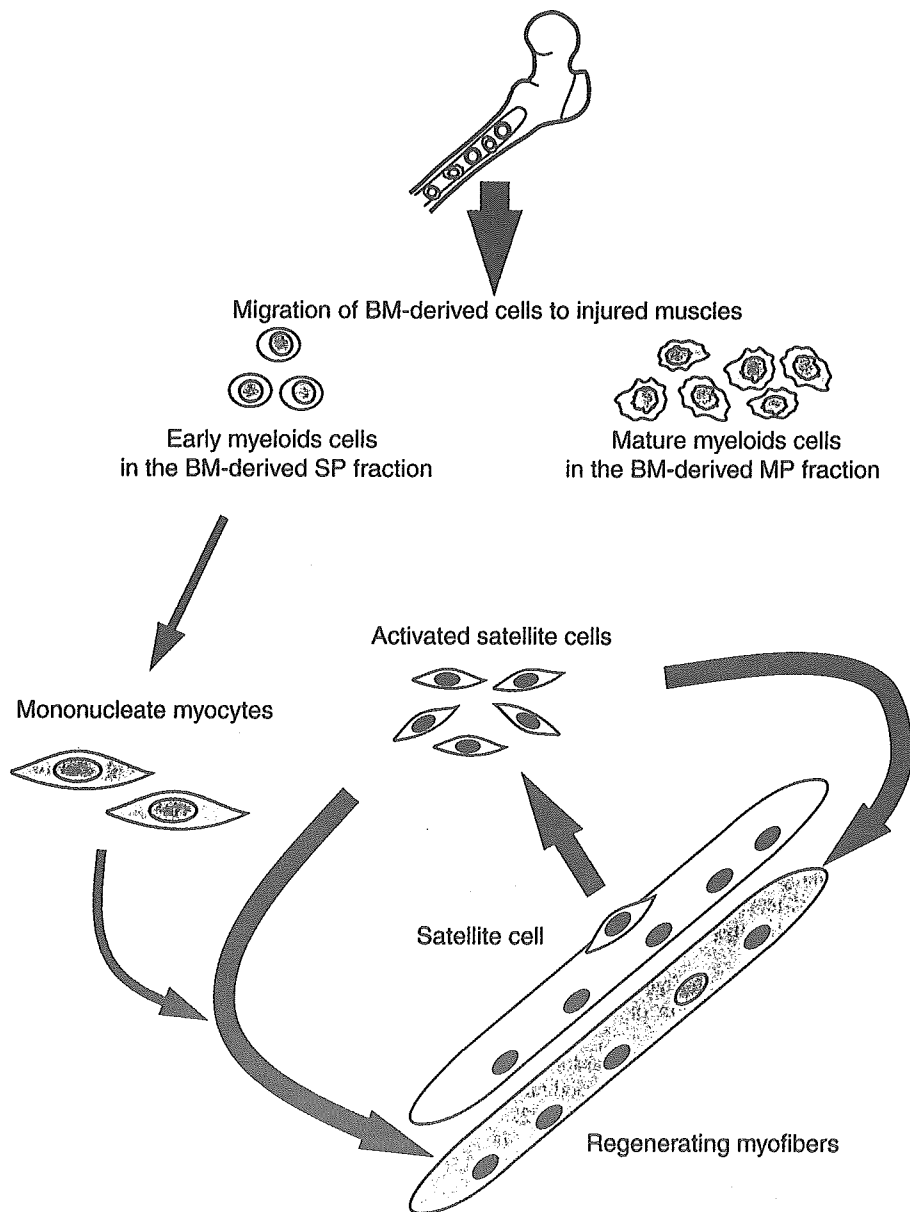


Fig. 5. Model for BM-derived SP cell-mediated muscle regeneration. In response to injury, BM-derived cells are mobilized to injured muscles (gray arrows). Neither HSCs nor hematopoietic progenitors migrate to injured muscles. Migrated BM-derived SP cells in regenerating muscles contain early myeloid cells that enrich cells with myogenic differentiation. These early myeloid cells advance toward mature multinucleated myotubes/myofibers via a myogenic differentiation program before fusion with myogenic cells (blue arrows). On the other hand, some mature macrophages might be stochastically incorporated into myotubes/myofibers at low efficiency.

BM-derived SP cells contain early myeloid cells that enrich cells capable of myogenic differentiation. In regenerating muscles, they advance toward mononucleated myocytes before fusion with pre-existing myogenic cells. They probably require cell-to-cell contact with myogenic cells for skeletal muscle differentiation. The molecular mechanism by which skeletal muscle cells are induced to fuse with BM-derived SP cells and to differentiate BM-derived SP cells into myogenic cells remains to be determined.

### Acknowledgments

We are grateful to colleagues in our laboratory, in particular Dr. S. Fukada, for useful discussion and suggestions on this work. K.O. is supported by a Research Fellowship from the Japan Society for the Promotion of Science. This work is supported by Grants-in-Aid for Center of Excellence (COE), Research on Nervous and Mental Disorders (10B-1, 13B-1), and Health Sciences Research Grants for Research on the Human Genome and Gene Therapy (H10-genome-015, H13-genome-001) from the Ministry of Health, Labor and Welfare of Japan, and a Grant-in-Aid for Scientific Research (B) from the Ministry of Education, Science, Sports and Culture of Japan.

### References

- [1] I. Angulo, J. Rullas, J.A. Campillo, E. Obregon, A. Heath, M. Howard, M.A. Munoz-Fernandez, J.L. Subiza, Early myeloid cells are high producers of nitric oxide upon CD40 plus IFN-gamma stimulation through a mechanism dependent on endogenous TNF-alpha and IL-1alpha, *Eur. J. Immunol.* 30 (2000) 1263–1271.
- [2] R. Bischoff, Proliferation of muscle satellite cells on intact myofibers in culture, *Dev. Biol.* 115 (1986) 129–139.
- [3] R. Bischoff, The satellite cell and muscle regeneration, in: A.G. Myology, C. Engel, A. Franszini-Armstrong (Eds.), McGraw-Hill, New York, 1994, pp. 97–118.
- [4] R.E. Bittner, C. Schöfer, K. Weipoltshammer, S. Ivanova, B. Streubel, E. Hauser, M. Freilinger, H. Höger, A. Elbe-Bürger, F. Wachtler, Recruitment of bone-marrow-derived cells by skeletal muscle and cardiac muscle in adult dystrophic mdx mice, *Anat. Embryol.* 199 (1999) 391–396.
- [5] T.R. Brazelton, M. Nystrom, H.M. Blau, Significant differences among skeletal muscles in the incorporation of bone marrow-derived cells, *Dev. Biol.* 262 (2003) 64–74.
- [6] F.D. Camargo, R. Green, Y. Capetenoki, K.A. Jackson, M.A. Goodell, Single hematopoietic stem cells generate skeletal muscle through myeloid intermediates, *Nat. Med.* 9 (2003) 1520–1527.
- [7] R.F. Castro, K.A. Jackson, M.A. Goodell, C.S. Robertson, H. Liu, H.D. Shine, Failure of bone marrow cells to transdifferentiate into neural cells in vivo, *Science* 297 (2002) 1299.
- [8] S.Y. Corbel, A. Lee, J. Duenas, T.R. Brazelton, H.M. Blau, F.M. Rossi, Contribution of hematopoietic stem cells to skeletal muscle, *Nat. Med.* 9 (2003) 1528–1532.
- [9] R. Couteaux, J.-C. Mira, A. d'Albis, Regeneration of muscles after cardiotoxin injury. I. Cytological aspects, *Biol. Cell* 62 (1988) 171–182.
- [10] L.D. De Angelis, L. Berghella, M. Coletta, L. Lattanzi, M. Zanchi, M.G.C. De Angelis, C. Ponzetto, G. Cossu, Skeletal myogenic progenitors originating from embryonic dorsal aorta coexpress endothelial and myogenic markers and contribute to postnatal muscle growth and regeneration, *J. Cell Biol.* 147 (1999) 869–877.
- [11] C.D. De Bari, F. Dell'Accio, F. Vandenabeele, J.R. Vermeesch, J.-M. Raymackers, F.P. Luyten, Skeletal muscle repair by adult human mesenchymal stem cells from synovial membrane, *J. Cell Biol.* 160 (2003) 909–918.
- [12] G. Ferrari, M.G.C. De Angelis, M. Coletta, E. Paolucci, A. Stornaiuolo, G. Cossu, F. Mavilio, Muscle regeneration by bone marrow-derived myogenic progenitors, *Science* 279 (1998) 1528–1530.
- [13] G. Ferrari, A. Stornaiuolo, F. Mavilio, Failure to correct murine muscular dystrophy, *Nature* 411 (2001) 1014–1015.
- [14] J.E. Fletcher, M.-S. Jiang, Possible mechanisms of action of cobra snake venom cardiotoxins and bee venom melittin, *Toxicon* 31 (1993) 669–695.
- [15] S. Fukada, Y. Miyagoe-Suzuki, H. Tsukihara, K. Yuasa, S. Higuchi, S. Ono, K. Tsujikawa, S. Takeda, H. Yamamoto, Muscle regeneration by reconstitution with bone marrow or fetal liver cells from green fluorescent protein-gene mice, *J. Cell Sci.* 115 (2002) 1285–1293.
- [16] M.A. Goodell, K. Brose, G. Paradis, A.S. Conner, R.C. Mulligan, Isolation and functional properties of murine hematopoietic stem cells that are replicating in vitro, *J. Exp. Med.* 183 (1996) 1797–1806.
- [17] M.A. Goodell, M. Rosenzweig, H. Kim, D.F. Marks, M. DeMaria, G. Paradis, S.A. Grupp, C.A. Sieff, R.C. Mulligan, R.P. Johnson, Dye efflux studies suggest that hematopoietic stem cells expressing low or undetectable levels of CD34 antigen exist in multiple species, *Nat. Med.* 3 (1997) 1337–1345.
- [18] E. Gussoni, Y. Soneoka, C.D. Strickland, E.A. Buzney, M.K. Khan, A.F. Flint, L.M. Kunkel, R.C. Mulligan, Dystrophin expression in the mdx mouse restored by stem cell transplantation, *Nature* 401 (1999) 390–394.
- [19] A. Hirata, S. Masuda, T. Tamura, K. Kai, K. Ojima, A. Fukase, K. Motoyoshi, K. Kamakura, Y. Miyagoe-Suzuki, S. Takeda, Expression profiling of cytokines and related genes in regenerating skeletal muscle after cardiotoxin injection: a role for osteopontin, *Am. J. Pathol.* 163 (2003) 203–215.
- [20] K.A. Jackson, T. Mi, M. Goodell, Hematopoietic potential of stem cells isolated from murine skeletal muscle, *Proc. Natl. Acad. Sci. USA* 96 (1999) 14482–14486.
- [21] H. Kawada, M. Ogawa, Bone marrow origin of hematopoietic progenitors and stem cells in murine muscle, *Blood* 98 (2001) 2008–2013.
- [22] M.A. LaBarge, H.M. Blau, Biological progression from adult bone marrow to mononucleate muscle stem cell to multinucleate muscle fiber in response to injury, *Cell* 111 (2002) 589–601.
- [23] S.L. McKinney-Freeman, S.M. Majka, K.A. Jackson, K. Norwood, K.K. Hirschi, M.A. Goodell, Altered phenotype and reduced function of muscle-derived hematopoietic stem cells, *Exp. Hematol.* 31 (2003) 806–814.
- [24] F. Montanaro, K. Liadaki, J. Volinski, A. Flint, L.M. Kunkel, Skeletal muscle engraftment potential of adult mouse skin side population cells, *Proc. Natl. Acad. Sci. USA* 100 (2003) 9336–9341.
- [25] A. Musarò, C. Giacinti, G. Borsellino, G. Dobrowolny, L. Pelosi, L. Cairns, S. Ottolenghi, G. Cossu, G. Bernardi, L. Battistini, M. Molinaro, N. Rosenthal, Stem cell-mediated muscle regeneration is enhanced by local isoform of insulin-like growth factor 1, *Proc. Natl. Acad. Sci. USA* 101 (2004) 1206–1210.
- [26] M. Ogawa, Y. Matsuzaki, S. Nishikawa, S. Hayashi, T. Kunisada, T. Sudo, T. Kina, H. Nakauchi, S. Nishikawa, Expression and function of c-kit in hemopoietic progenitor cells, *J. Exp. Med.* 174 (1991) 63–71.

- [27] M. Okabe, M. Ikawa, K. Kōminami, T. Nakanishi, Y. Nishimune, 'Green mice' as a source of ubiquitous green cells, *FEBS Lett.* 407 (1997) 313–319.
- [28] D.J. Pearce, C.M. Ridler, C. Simpson, D. Bonnet, Multi-parameter analysis of murine bone marrow side population cells, *Blood* (2003).
- [29] P. Ralph, M.-K. Ho, P.B. Litcofsky, T.A. Springer, Expression and induction in vitro of macrophage differentiation antigens on murine cell lines, *J. Immunol.* 130 (1983) 108–114.
- [30] T. Reya, N.V. Contractor, M.S. Couzens, M.A. Wasik, S.G. Emerson, S.R. Carding, Abnormal myelocytic cell development in interleukin-2 (IL-2)-deficient mice: evidence for the involvement of IL-2 in myelopoiesis, *Blood* 91 (1998) 2935–2947.
- [31] J.D. Rosenblatt, A.I. Lunt, D.J. Parry, T.A. Partridge, Culturing satellite cells from living single muscle fiber explants, *In Vitro Cell. Dev. Biol.-Animal.* 31 (1995) 773–779.
- [32] C.W. Scharenberg, M.A. Harkey, B. Torok-Storb, The ABCG2 transporter is an efficient Hoechst 33342 efflux pump and is preferentially expressed by immature human hematopoietic progenitors, *Blood* 99 (2002) 507–512.
- [33] P. Seale, M.A. Rudnicki, A new look at the origin, function, and stem-cell status of muscle satellite cells, *Dev. Biol.* 218 (2000) 115–124.
- [34] I.S. Trowbridge, M.L. Thomas, CD45: an emerging role as a protein tyrosine phosphatase required for lymphocyte activation and development, *Annu. Rev. Immunol.* 12 (1994) 85–116.
- [35] S. Wakitani, T. Saito, A.I. Caplan, Myogenic cells derived from rat bone marrow mesenchymal stem cells exposed to 5-azacytidine, *Muscle Nerve* 18 (1995) 1417–1426.
- [36] M. Ye, H. Iwasaki, C.V. Laiosa, M. Stadtfeld, H. Xie, S. Heck, B. Clausen, K. Akashi, T. Graf, Hematopoietic stem cells expressing the myeloid lysozyme gene retain long-term, multilineage repopulation potential, *Immunity* 19 (2003) 689–699.
- [37] B.P. Zambrowicz, A. Imamoto, S. Fiering, L.A. Herzenberg, W.G. Kerr, P. Soriano, Disruption of overlapping transcripts in the ROSA  $\beta$ geo 26 gene trap strain leads to widespread expression of  $\beta$ -galactosidase in mouse embryos and hematopoietic cells, *Proc. Natl. Acad. Sci. USA* 94 (1997) 3489–3794.
- [38] P.S. Zammit, L. Heslop, V. Hudon, J.D. Rosenblatt, S. Tajbakhsh, M.E. Buckingham, J.R. Beauchamp, T.A. Partridge, Kinetics of myoblast proliferation show that resident satellite cells are competent to fully regenerate skeletal muscle fibers, *Exp. Cell Res.* 281 (2002) 39–49.
- [39] Y. Zhao, D. Glesne, E. Huberman, A human peripheral blood monocyte-derived subset acts as pluripotent stem cells, *Proc. Natl. Acad. Sci. USA* 100 (2003) 2426–2431.

## Purification and cell-surface marker characterization of quiescent satellite cells from murine skeletal muscle by a novel monoclonal antibody

So-ichiro Fukada,<sup>a</sup> Saito Higuchi,<sup>a</sup> Masashi Segawa,<sup>a</sup> Ken-ichi Koda,<sup>a</sup> Yukiko Yamamoto,<sup>a</sup> Kazutake Tsujikawa,<sup>a</sup> Yasuhiro Kohama,<sup>a</sup> Akiyoshi Uezumi,<sup>b</sup> Michihiro Imamura,<sup>b</sup> Yuko Miyagoe-Suzuki,<sup>b</sup> Shin'ichi Takeda,<sup>b</sup> and Hiroshi Yamamoto<sup>a,\*</sup>

<sup>a</sup>Department of Immunology, Graduate School of Pharmaceutical Sciences, Osaka University, Suita, Osaka 565-0871, Japan

<sup>b</sup>Department of Molecular Therapy, National Institute of Neuroscience, National Center of Neurology and Psychiatry, Kodaira, Tokyo 187-8502, Japan

Received 10 November 2003; received in revised form 16 February 2004

Available online 25 March 2004

### Abstract

A novel monoclonal antibody, SM/C-2.6, specific for mouse muscle satellite cells was established. SM/C-2.6 detects mononucleated cells beneath the basal lamina of skeletal muscle, and the cells co-express M-cadherin. Single fiber analyses revealed that M-cadherin<sup>+</sup> mononucleated cells attaching to muscle fibers are stained with SM/C-2.6. SM/C-2.6<sup>+</sup> cells, which were freshly purified by FACS from mouse skeletal muscle, became MyoD<sup>+</sup> in vitro in proliferating medium, and the cells differentiated into desmin<sup>+</sup> and nuclear-MyoD<sup>+</sup> myofibers in vitro when placed under differentiation conditions. When the sorted cells were injected into *mdx* mouse muscles, donor cells differentiated into muscle fibers. Flow cytometric analyses of SM/C-2.6<sup>+</sup> cells showed that the quiescent satellite cells were c-kit<sup>-</sup>, Sca-1<sup>-</sup>, CD34<sup>+</sup>, and CD45<sup>-</sup>. More, SM/C-2.6<sup>+</sup> cells were barely included in the side population but in the main population of cells in Hoechst dye efflux assay. These results suggest that SM/C-2.6 identifies and enriches quiescent satellite cells from adult mouse muscle, and that the antibody will be useful as a powerful tool for the characterization of cellular and molecular mechanisms of satellite cell activation and proliferation.

© 2004 Elsevier Inc. All rights reserved.

**Keywords:** Cell surface marker; Satellite cell; Skeletal muscle; Stem cell

### Introduction

During the last decade, many reports have described the existence of tissue-specific stem cells that are able to self-renew and generate committed progenitors. Hematopoietic stem cells in bone marrow are well-characterized and defined as c-kit<sup>+</sup>, Sca-1<sup>+</sup>, and Lin<sup>-</sup> [1,2], and bone marrow transplantation is now clinically applied to various immunological and hematological disorders. In addition to hematopoietic stem cells, bone marrow contains mesenchymal stem cells that have been characterized by their ability to differentiate

into various types of tissue-specific cells in both in vitro and in vivo experiments. Mesenchymal stem cells can generate bone, cartilage, connective tissue [3–7], and cardiomyocytes [8]. Cord blood also contains mesenchymal stem cells [9–11] and this also forms various mesenchymal tissue cells in vitro.

It is widely accepted that the postnatal growth and repair of skeletal muscle is normally mediated by satellite cells that locate between the basal lamina and sarcolemma of myofibers [12–14]. Thus, satellite cells have been considered to be the only myogenic source for the maintenance of skeletal muscle [15,16]. Satellite cells can be enriched by culturing cells from enzymatically digested muscles [17–21]. When muscle regeneration starts, the state of the satellite cells changes from resting or quiescent to activated and proliferative. However, the conditions under which the activation and the proliferation of satellite cells are initiated have not yet been well characterized.

The myogenic potential of mesenchymal stem cells from rat bone marrow in both in vivo [22] and in vitro experiments [23] has been described. These results prompted speculation

**Abbreviations:** GFP-Tg, Green fluorescent protein gene transgenic; MAb, Monoclonal antibody; MP, Main population; SP, Side population; TA, Tibialis anterior.

\* Corresponding author. Department of Immunology, Graduate School of Pharmaceutical Sciences, Osaka University, 1-6 Yamada-oka, Suita, Osaka 565-0871, Japan. Fax: +81-6-6879-8194.

E-mail address: [hiroshiy@phs.osaka-u.ac.jp](mailto:hiroshiy@phs.osaka-u.ac.jp) (H. Yamamoto).